Supporting Information

for

pH-Responsive N^C-cyclometalated iridium(III) complexes: synthesis, photophysical properties, computational results, and bioimaging application

Anastasia I. Solomatina*, Daria O. Kozina, Vitaly V. Porsev*, Sergey P. Tunik*

Institute of Chemistry, St. Petersburg State University, Universitetskii av., 26, 198504 St. Petersburg, Russia; nastisol@gmail.com (A.I.S.); kozina.d@yandex.ru (D.O.K.); v.porsev@spbu.ru (V.V.P.); sergey.tunik@spbu.ru (S.P.T.)

Content

Part 1. XRD-analysis, NMR spectroscopy and ESI mass-spectrometry data

*Table S1. Selected bond distances (Å) and angles (°) in the structure of **2**.*

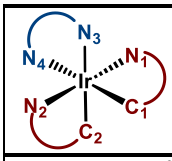					
Distances, Å		Angles, °		Angles, °	
Ir-C1	2.005(6)	N1-Ir-C1	79.7(2)	C1-Ir-N2	97.0(2)
Ir-N1	2.040(5)	N2-Ir-C2	80.2(2)	N2-Ir-N4	88.13(18)
Ir-C2	2.016(5)	N3-Ir-N4	77.1(2)	N4-Ir-N1	95.4(2)
Ir-N2	2.075(5)	C1-Ir-C2	85.7(2)	N3-Ir-N2	96.5(2)
Ir-N3	2.132(4)	C2-Ir-N1	97.2(2)	N3-Ir-N1	86.23(17)
Ir-N4	2.128(5)	C2-Ir-N4	99.3(2)	N3-Ir-C1	98.2(2)

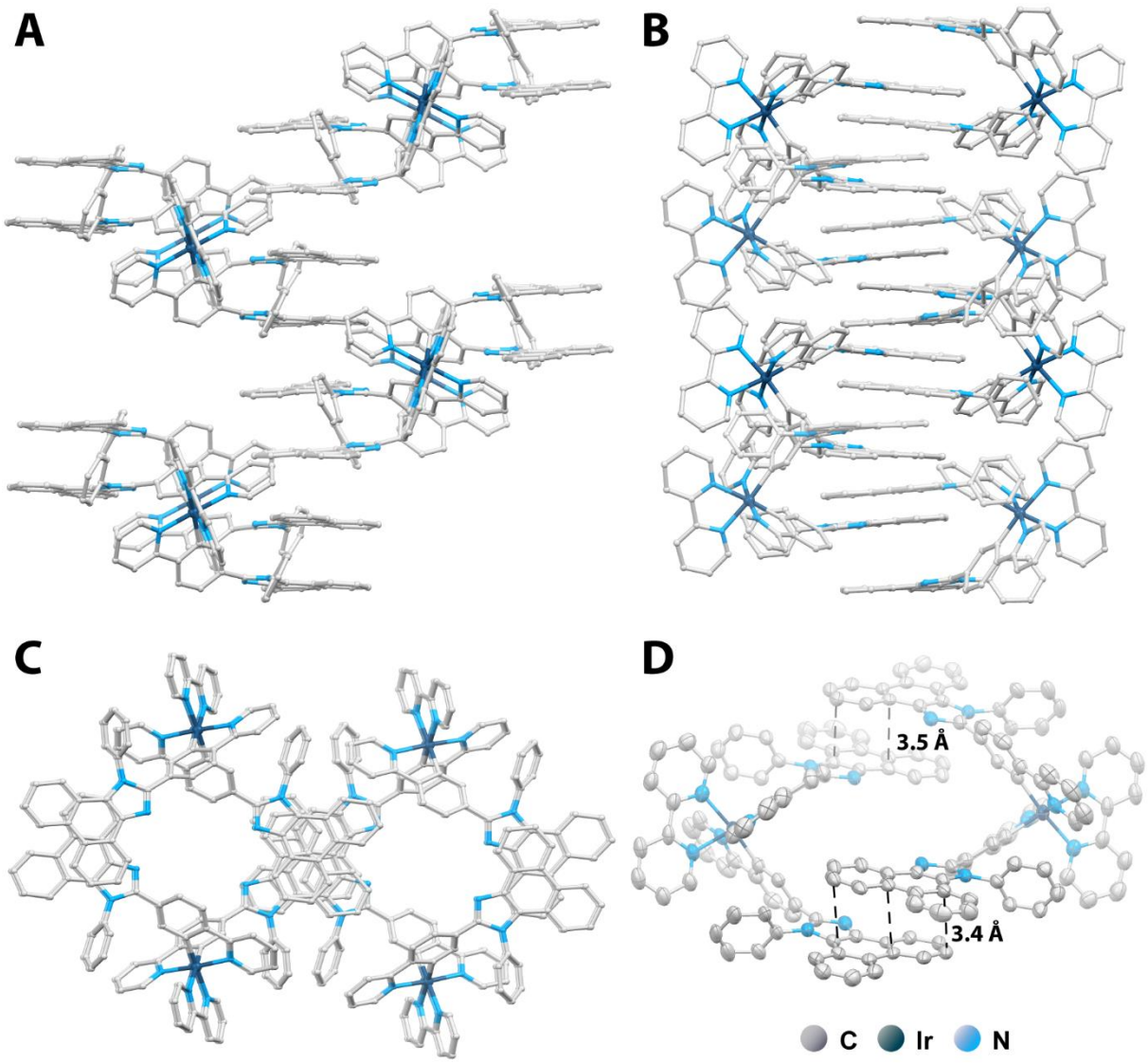

*Figure S1. Perspective view of **2** packing in the solid state: A – front view, B – right view, C – top view, D – short π-π interactions between phenanthrene moieties showing thermal ellipsoids at the 40% probability level (H-atoms are omitted for clarity).*

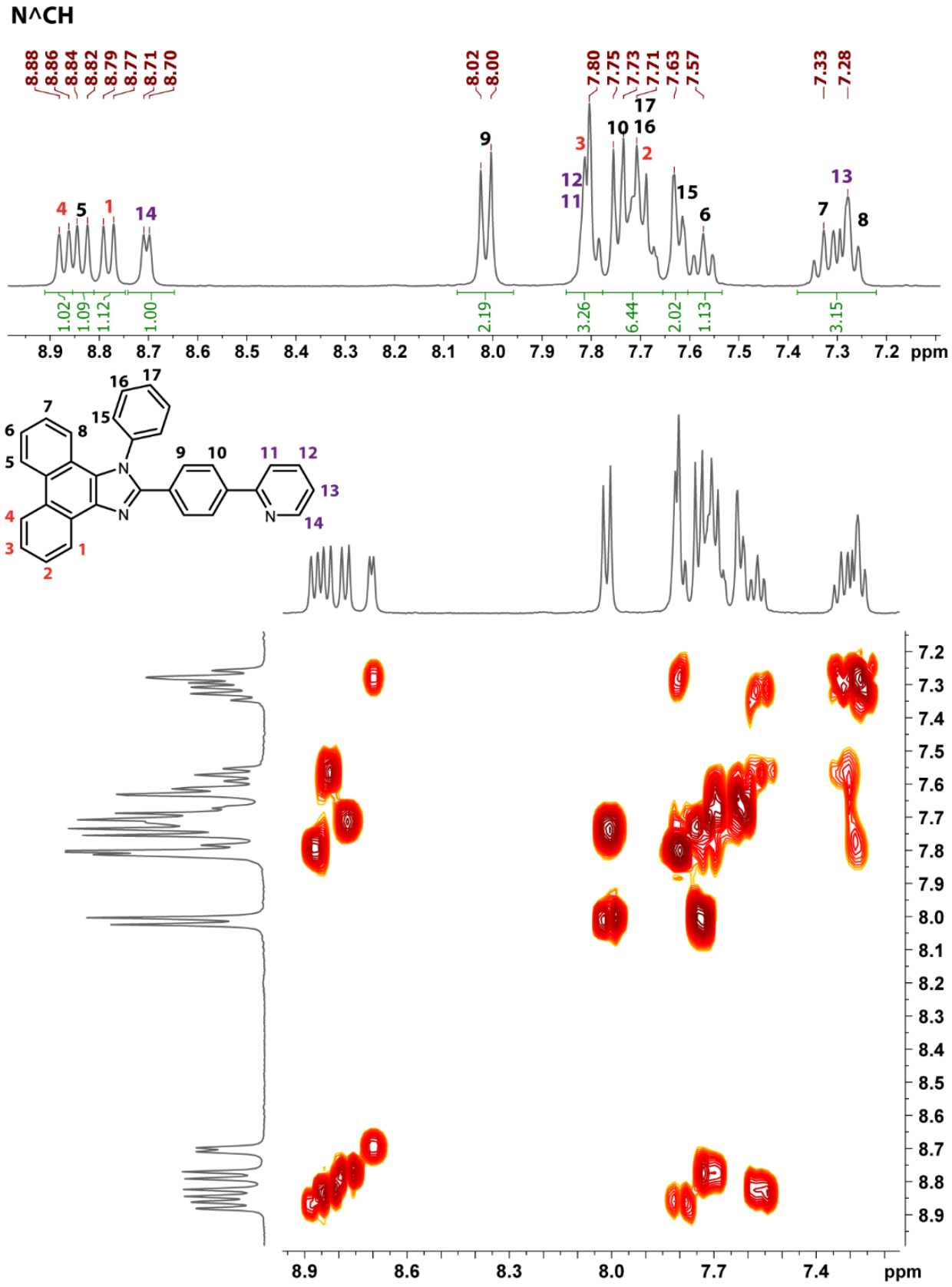

*Figure S2. ^{1}H and ^{1}H-^{1}H COSY NMR spectrum of **N^CH** in CD_2Cl_2, 298 K.*

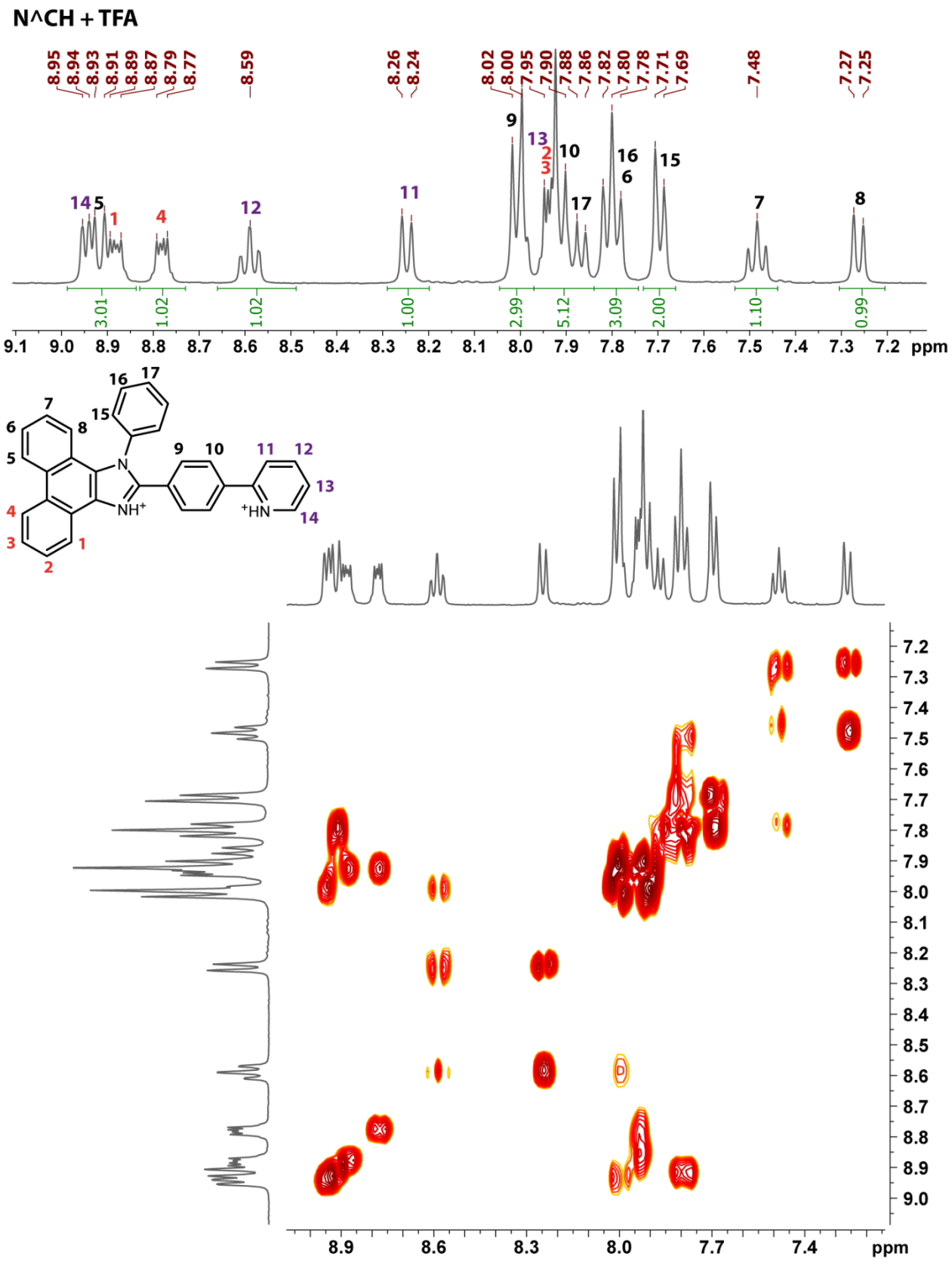

*Figure S3. ^{1}H and ^{1}H-^{1}H COSY NMR spectrum of **N^CH** in CD_2Cl_2 with TFA, 298 K.*

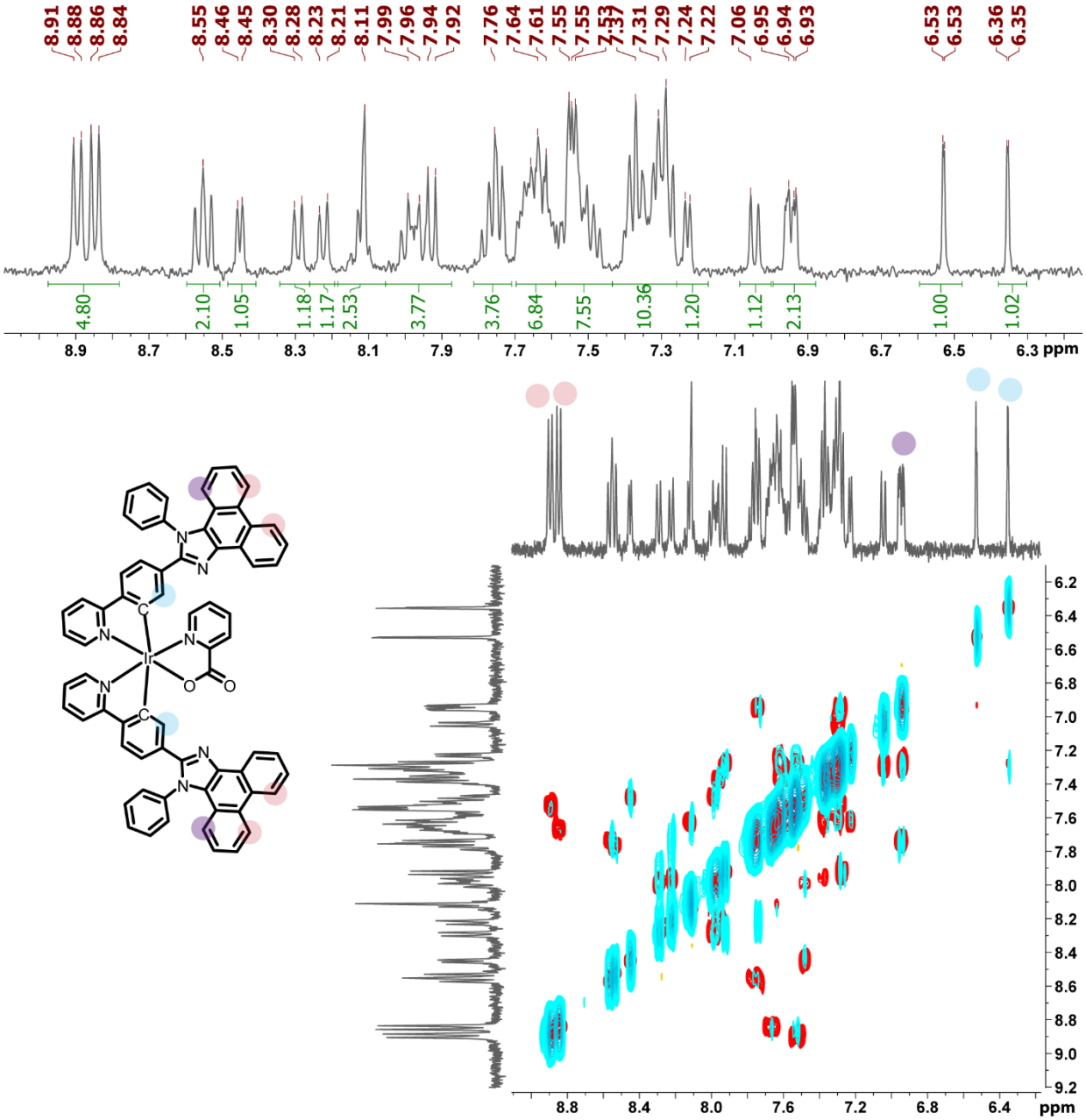

*Figure S4. ^{1}H and overlapped ^{1}H-^{1}H COSY and NOESY NMR spectra of complex **1** with assignment (given by different colours at the spectrum and structural pattern) of some signals to protons, DMSO-d6, 298 K.*

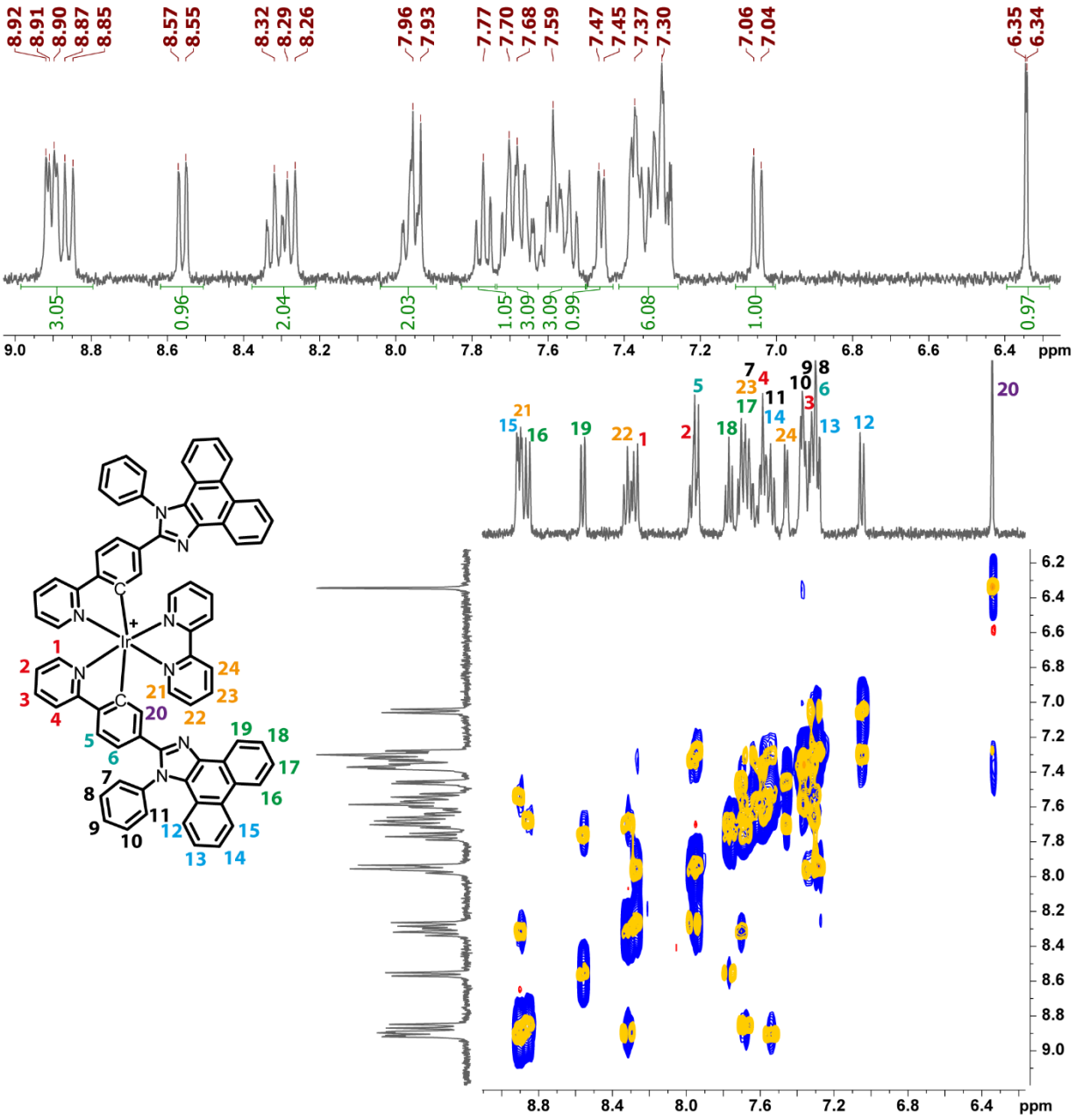

*Figure S5. ^{1}H and overlapped ^{1}H-^{1}H COSY and NOESY NMR spectra of complex **2** with full assignment of the signals to protons, DMSO-d6, 298 K.*

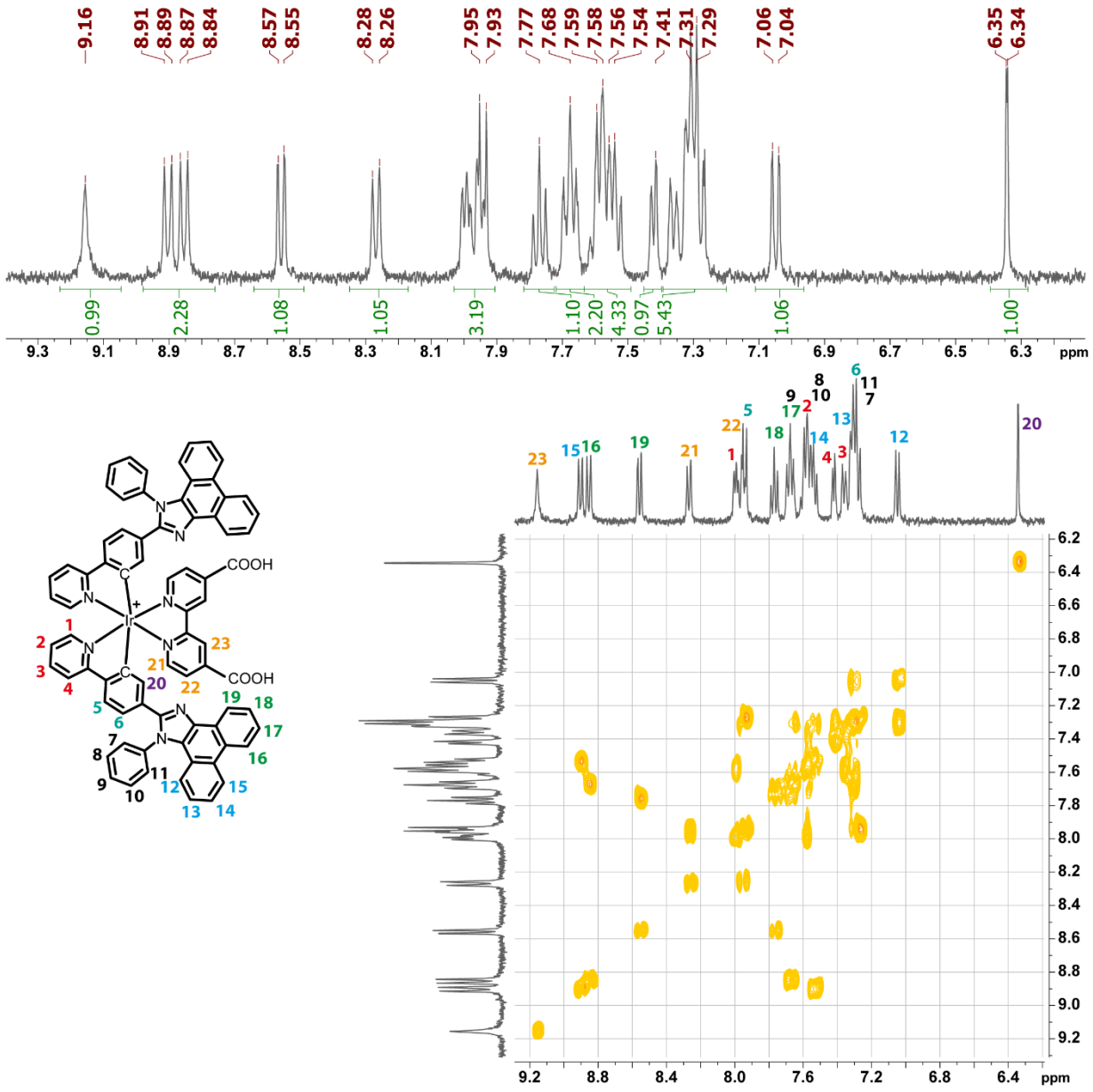

*Figure S6. ^{1}H and ^{1}H-^{1}H COSY NMR spectra of complex **3** with full assignment of the signals to protons, DMSO-d6, 298 K.*

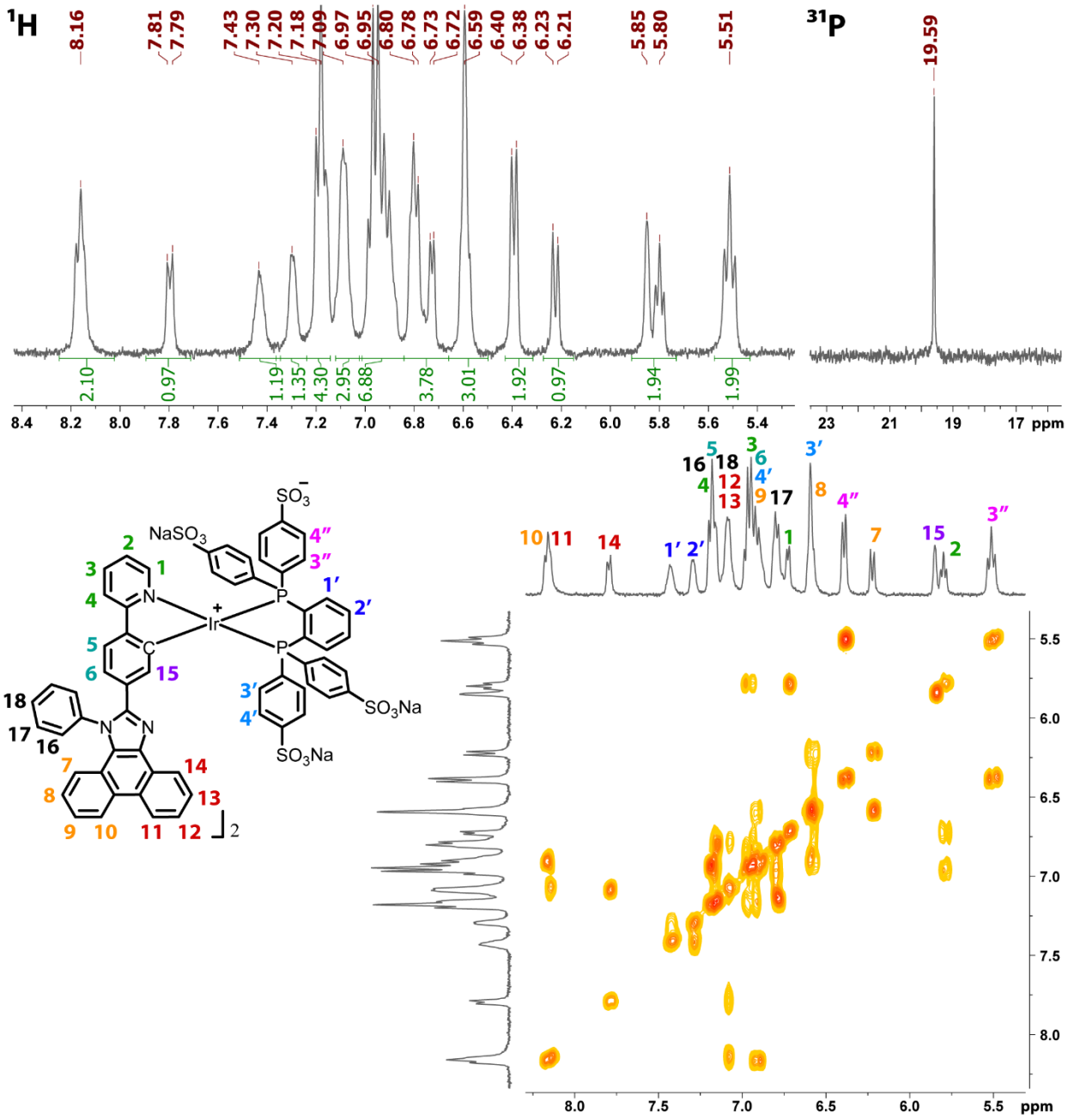

*Figure S7. ^{1}H and ^{31}P NMR spectra and ^{1}H-^{1}H COSY NMR spectra of complex **4** with full assignment of the signals to protons, DMSO-d6, 298 K.*

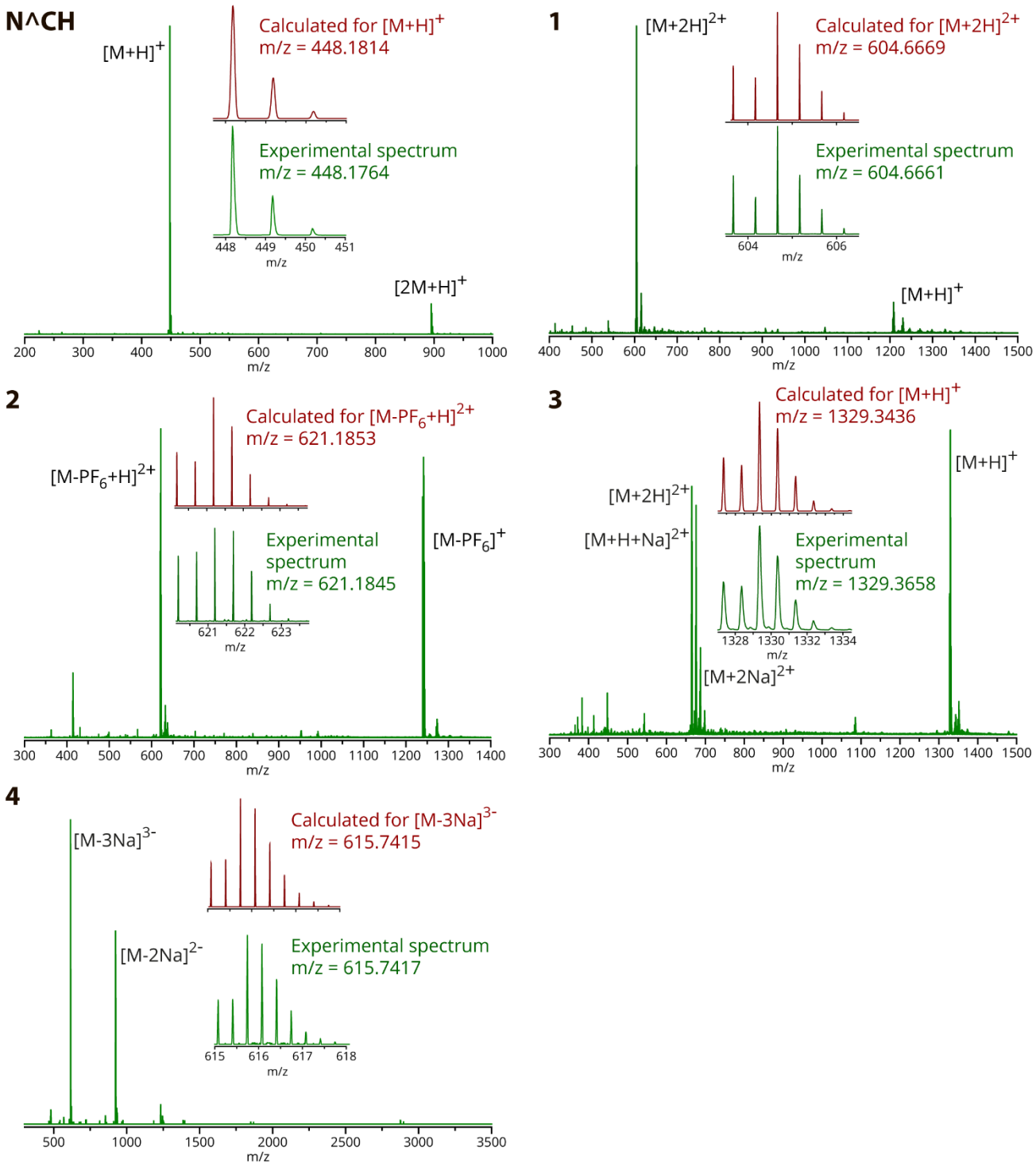

*Figure S8. Experimental and calculated ESI mass spectra of **1-4** and **N^CH**.*

Part 2. Photophysical properties of complexes 1-4 and N^CH

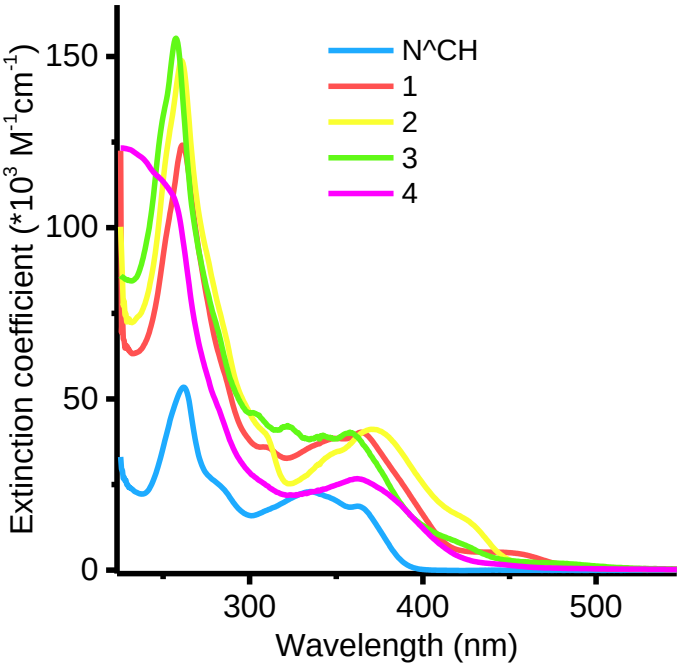

*Figure S9. Absorption spectra of **N^CH** and complexes **1, 2** in CH_2Cl_2, **3** in CH_3OH, and **4** in water, 298 K.*

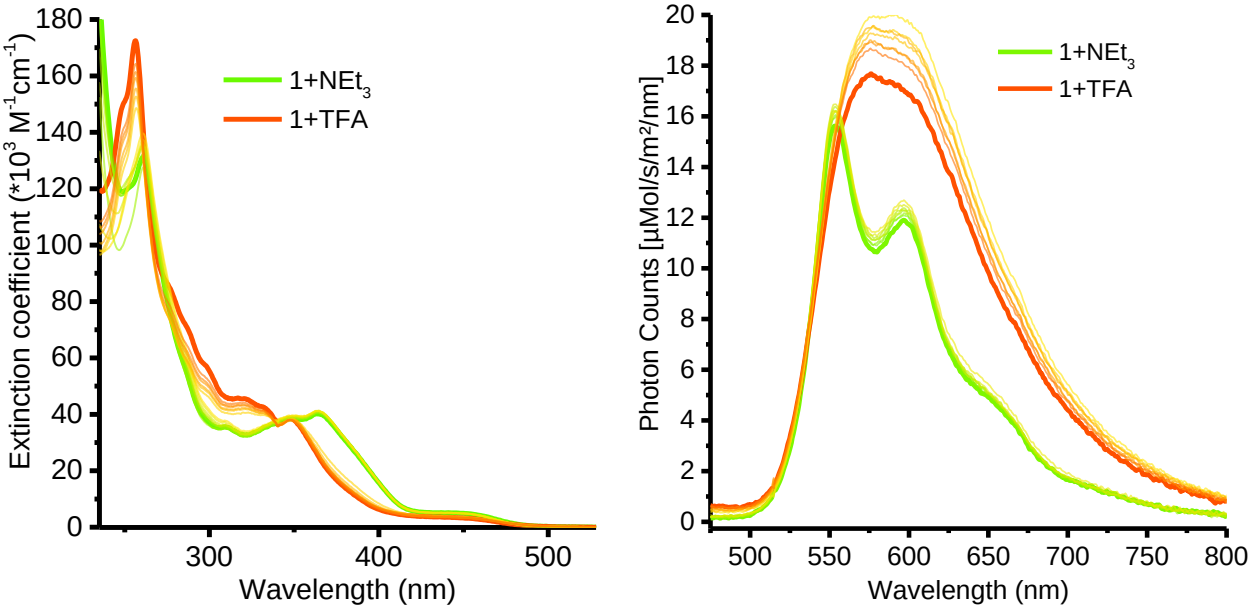

*Figure S10. Absorption (left) and emission (right) spectra of complex **1** in CH_2Cl_2 upon addition of base (NEt_3, green) or acid (THF, red), 298 K.*

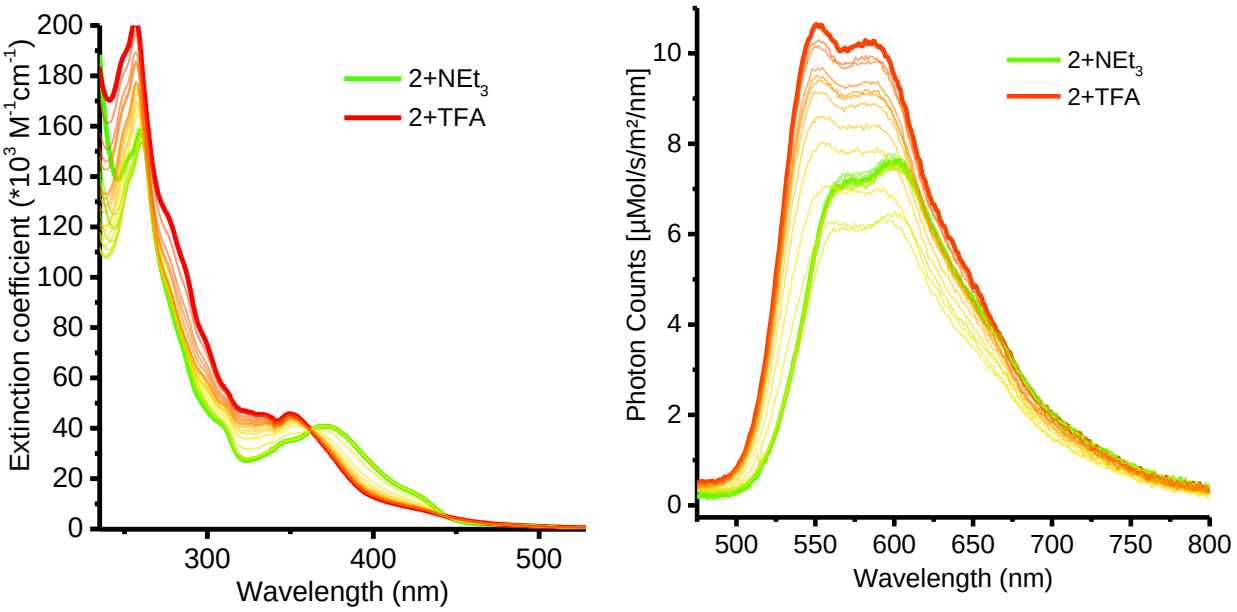

*Figure S11. Absorption (left) and emission (right) spectra of complex **2** in CH_2Cl_2 upon addition of base (NEt_3, green) or acid (THF, red), 298 K.*

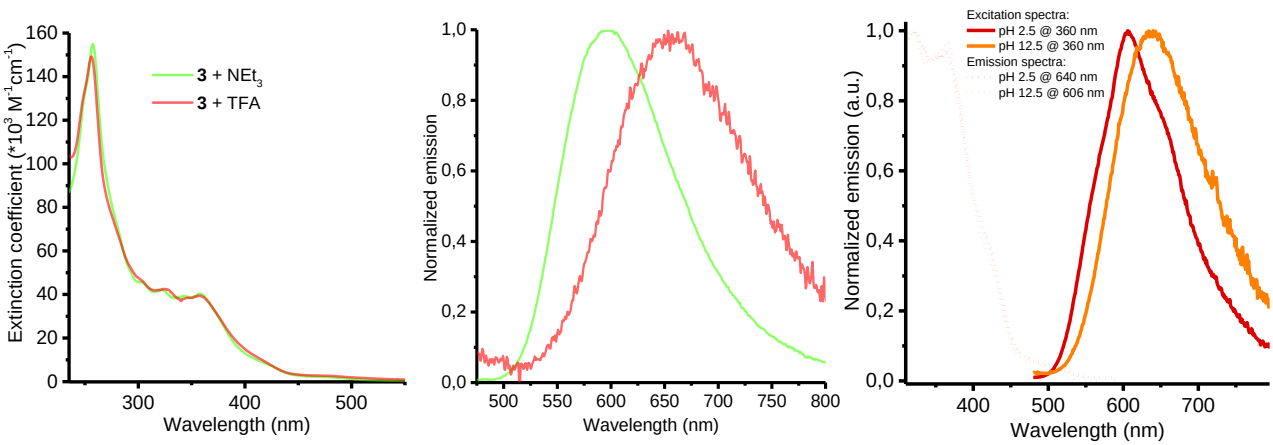

*Figure S12. Absorption (left) and emission (center) spectra of complex **3** in MeOH upon addition of base (NEt_3, green) or acid (TFA, red). Right: excitation (dashed) and emission (solid) spectra of complex 3 in aqueous buffer solutions at pH 2.5 and 12.5, 298 K, aerated solutions.*

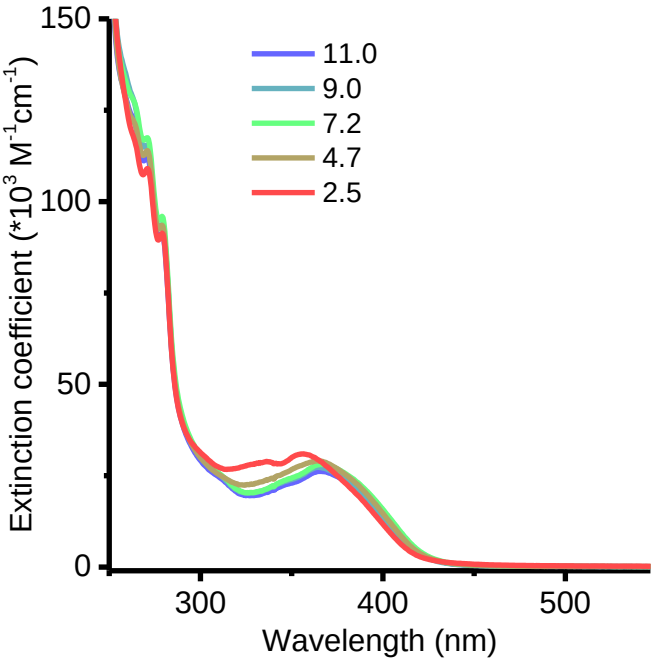

*Figure S13. Absorption spectra of **4** in aqueous buffer solutions with different pH, 298 K.*

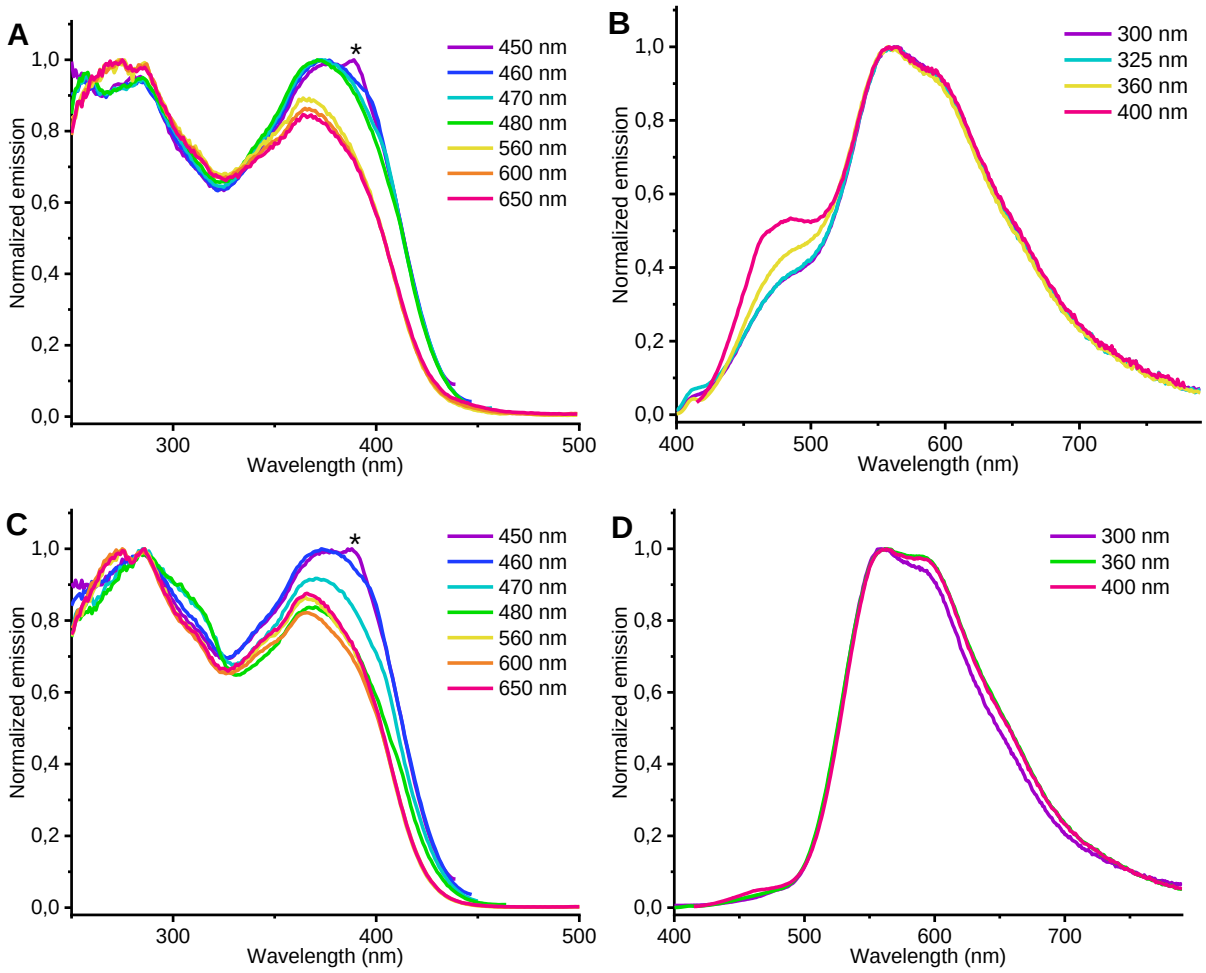

*Figure S14. Excitation (A, C) and emission (B, D) spectra of **4** in 0.1 M NaOH aqueous air-saturated (A, B) and Ar-saturated (C, D) solutions, 298 K. The asterisks denote the Raman peak of water.*

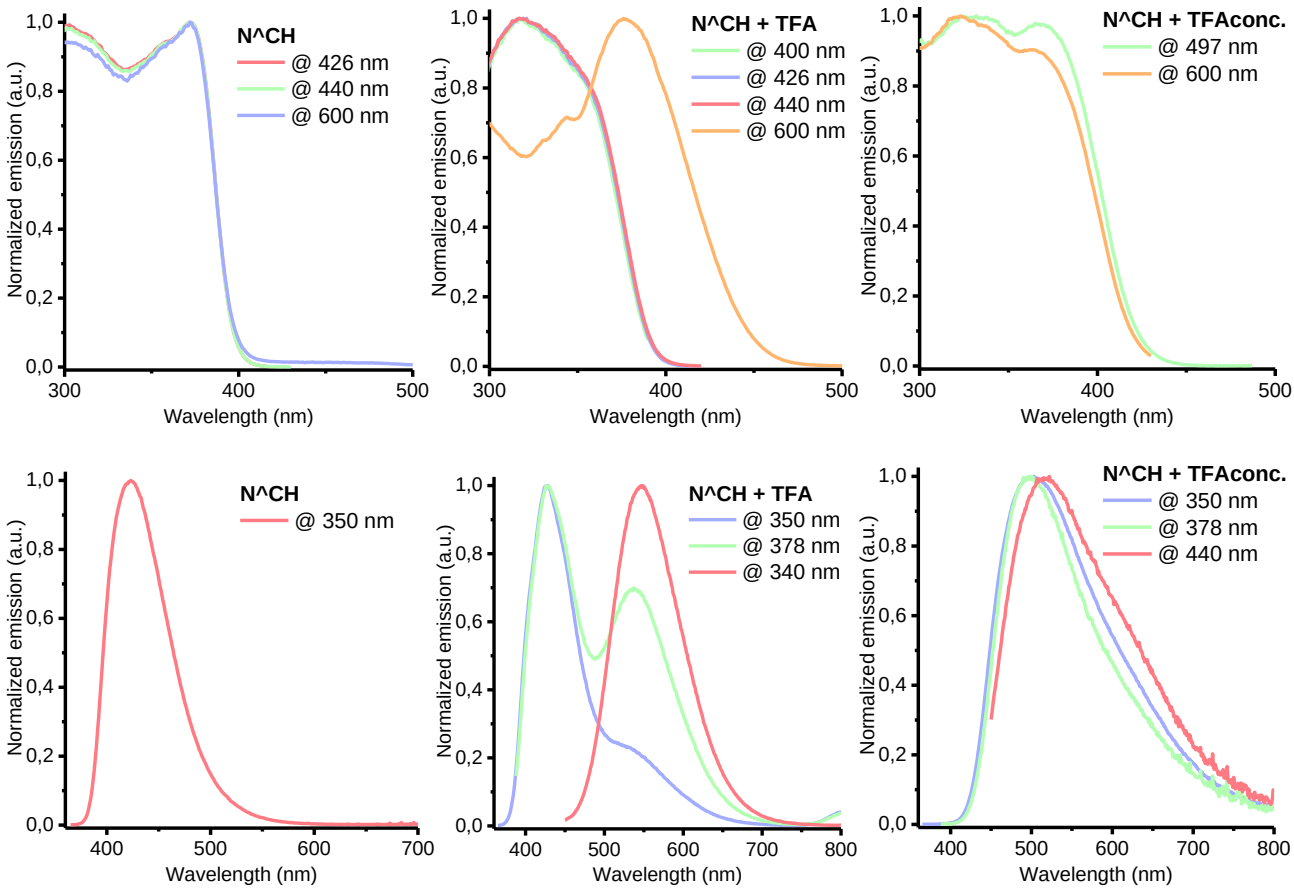

*Figure S15. Excitation (top) and emission (bottom) spectra of **N^CH** in CH_2Cl_2 upon addition of TFA, 298 K.*

Part 3. Computational results

*Table S2. Experimental and calculated photophysical properties of **N^CH** and complexes **1** and **2** in CH_2Cl_2, complex **3** in CH_3OH, and complex **4** in water.*

Complex	Abs, nm ($\varepsilon*10^{-4}$, $L*mol^{-1}*cm^{-1}$)		λ_{em}, nm	
	exp	calc	exp	calc
1	261 (124), 308sh (36), 350sh (38), 364 (40), 450sh (5)	255 (139), 288sh (65), 373 (55), 427sh (19)	554, 597, 650sh	534
{**1**+2H$^+$}	256, 277sh, 298sh, 320sh, 333sh, 348, 450sh	250 (121), 279sh (68), 357 (75), 437sh (15)	590	559
2	260 (149), 309sh (40), 350sh (34), 370 (41), 425sh (15)	255 (172), 288sh (75), 320sh (35), 395 (50)	570, 600, 650sh	517
{**2**+2H$^+$}	257, 275sh, 300sh, 310sh, 335sh, 350sh, 425sh	249 (151), 275sh (86), 293sh (67), 364 (73), 408sh (25)	550, 585, 640sh	484
4	264sh (122), 270 (112), 279 (91), 308sh (25), 366 (26)	254 (186), 296sh (46), 317sh (31), 393 (72)	482sh, 555, 587sh	531
{**4**+2H$^+$}	264sh (117), 271 (110), 279 (91), 356 (31)	250 (148), 284 (60), 373 (69)	563	536
{**3**−2H$^+$}	258 (155), 304 (45), 322 (42), 342 (39), 357 (40), 420sh (8), 480sh (2)	253 (194), 288sh (72), 335sh (30), 357sh (46), 373 (61), 401sh (36)	595	466
{**3**+2H$^+$}	255 (148), 301sh (47), 325 (42), 357 (40), 420sh (9), 480sh (2)	250 (126), 287 (74), 359 (71)	650	556
N^CH	262 (53), 280 (25), 335 (23), 363 (19)	254 (59), 268 (55), 291sh (25), 352 (56)	423	406

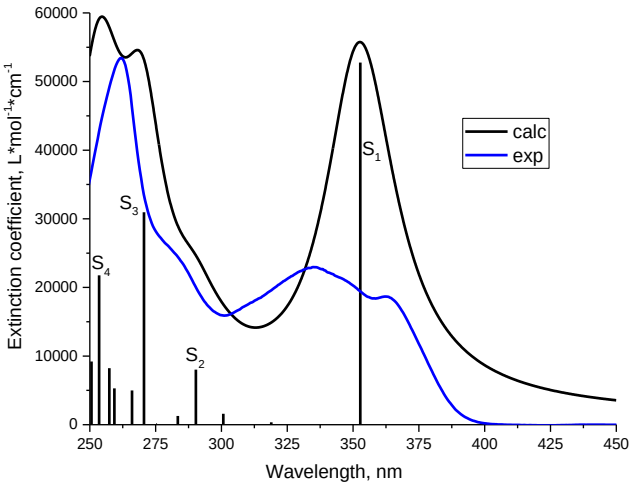

*Figure S16. Absorption spectra of **N^CH** in CH_2Cl_2 solution: experimental (blue) and calculated (black) lines with oscillator strengths of electronic transitions (bars).*

*Table S3. Experimental and calculated absorption maxima (λ), extinction coefficients (ε), oscillator strengths (f) of **N^CH.***

λ_{abs}, nm (exp)	$\varepsilon*10^{-3}$, $L*mol^{-1}*cm^{-1}$ (exp)	Transitions	λ_{abs}, nm (calc)	*f* (calc)	Contribution of main NTO pair in transition (%)
261	53	S_0-S_4	254	0.38	43
		S_0-S_3	271	0.55	85
284sh	24	S_0-S_2	290	0.14	52
335	23	S_0-S_1	353	0.93	97

*Table S4 The decrease (blue) and increase (red) in electron density for most intensive electronic absorption transitions of **N^CH**. The data for the corresponding interfragment charge transfer (IFCT) are given below the figures. Diagonal values represent intraligand transitions, off-diagonal values represent a charge transfer from "Donor" to "Acceptor". Fragments: PhPy – 2-phenylpyridine, Im – imidazole ring, phen – phenanthrene, Ph – phenyl ring.*

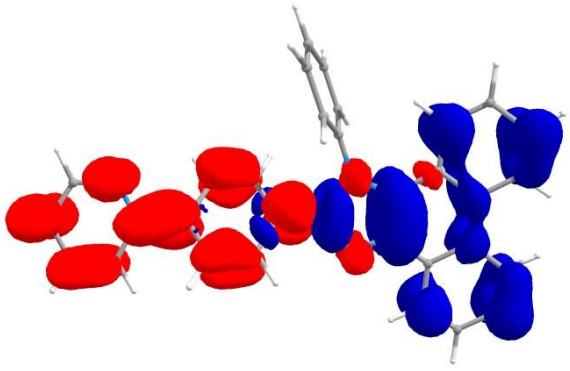

$S_0 \rightarrow S_1$

Donor	Acceptor			
	PhPy	Im	Ph	phen
PhPy	0.119	0.024	0.002	0.016
Im	0.310	0.062	0.006	0.041
Ph	0.004	0.001	0.000	0.001
phen	0.307	0.062	0.005	0.041

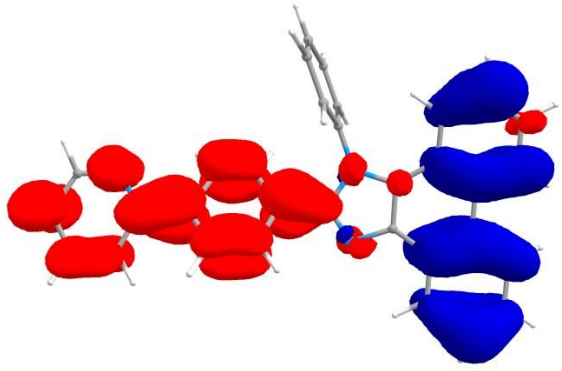

$S_0 \rightarrow S_2$

Donor	Acceptor			
	PhPy	Im	Ph	phen
PhPy	0.036	0.009	0.022	0.009
Im	0.107	0.027	0.067	0.026
Ph	0.003	0.001	0.002	0.001
phen	0.325	0.082	0.204	0.080

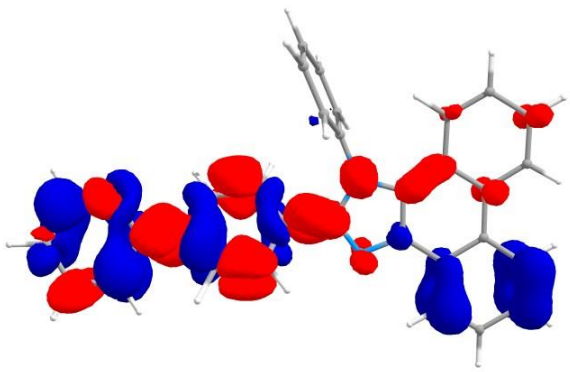

$S_0 \rightarrow S_3$

Donor	Acceptor			
	PhPy	Im	Ph	phen
PhPy	0.503	0.105	0.011	0.080
Im	0.047	0.010	0.001	0.007
Ph	0.013	0.003	0.000	0.002
phen	0.156	0.033	0.003	0.025

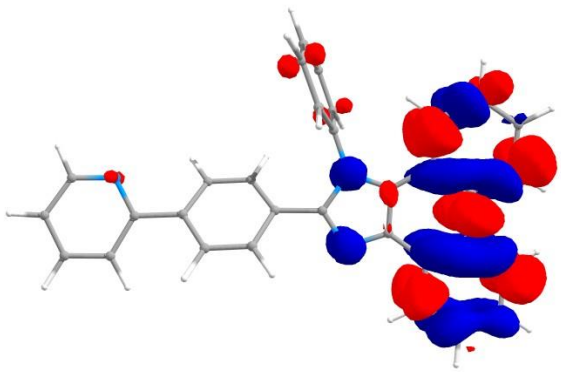

$S_0 \rightarrow S_4$

Donor	Acceptor			
	PhPy	Im	Ph	phen
PhPy	0.011	0.003	0.002	0.019
Im	0.047	0.013	0.008	0.081
Ph	0.054	0.015	0.009	0.093
phen	0.204	0.057	0.034	0.351

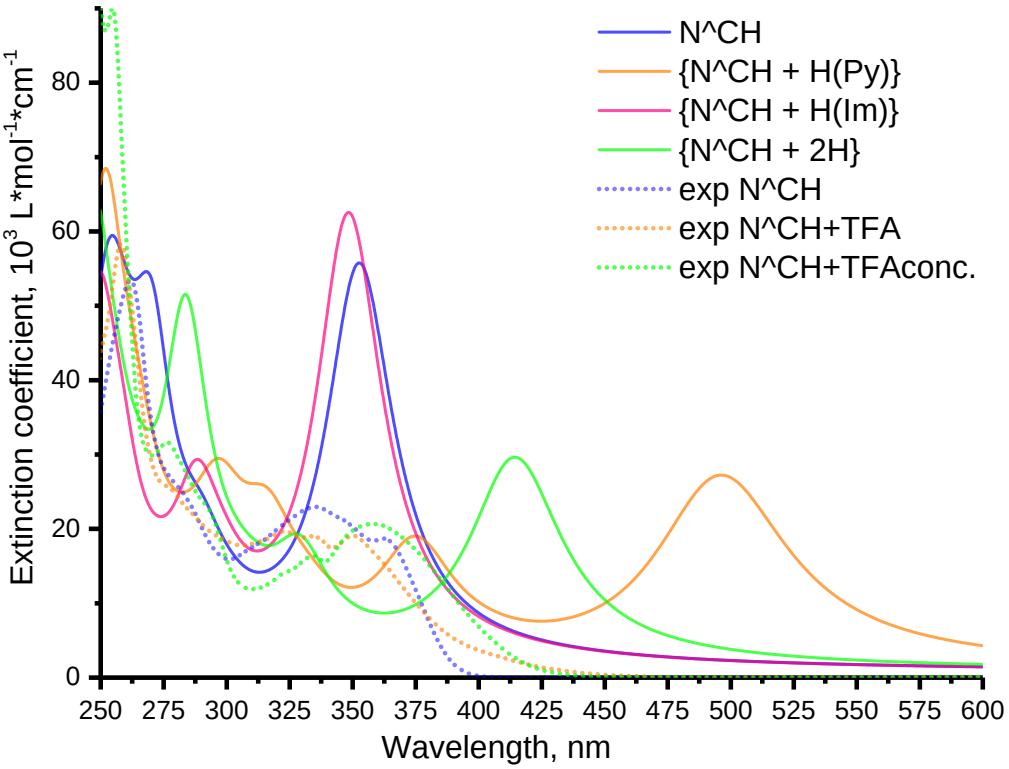

Figure S17. Experimental (dashed lines) and calculated (solid lines) absorption spectra of ***N^CH*** *and products of its protonation on pyridine {****N^CH*** *+ H^+(Py)}, imidazole {****N^CH*** *+ H^+(Im)}, and on both moieties {****N^CH*** *+ $2H^+$} in CH_2Cl_2.*

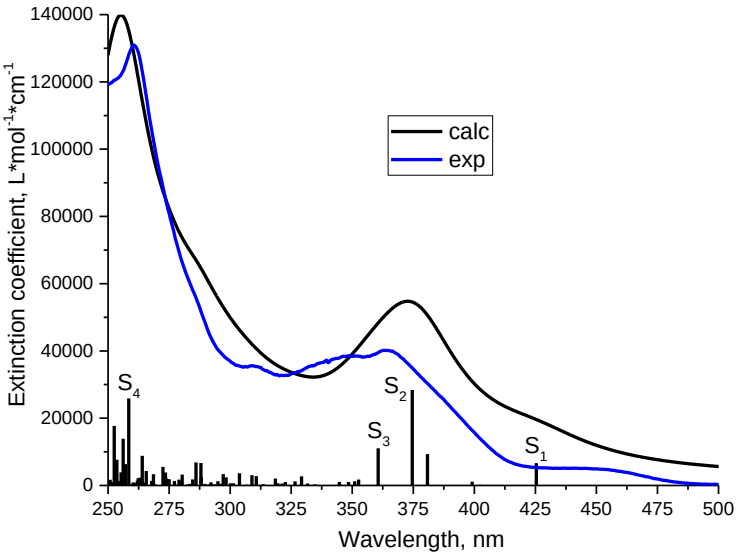

*Figure S18. Absorption spectra of complex **1** in CH_2Cl_2 solution: experimental (blue) and calculated (black) lines with oscillator strengths of electronic transitions (bars).*

*Table S5. Experimental and calculated absorption maxima (λ), extinction coefficients (ε), oscillator strengths (f) of **1**.*

Complex	λ_{abs}, nm (exp)	$\varepsilon*10^{-3}$, $L*mol^{-1}*cm^{-1}$ (exp)	Transitions	λ_{abs}, nm (calc)	*f* (calc)	Contribution of main NTO pair in transition (%)
1	261	124	S_0-S_4	258	0.53	39
	364	40	S_0-S_3	361	0.22	87
			S_0-S_2	375	0.58	90
	450sh	5	S_0-S_1	425	0.14	95

*Table S6. The decrease (blue) and increase (red) in electron density for most intensive electronic absorption transitions of **1**. The data for the corresponding interfragment charge transfer (IFCT) are given below the figures. Diagonal values represent intraligand transitions, off-diagonal values represent a charge transfer from "Donor" to "Acceptor".*

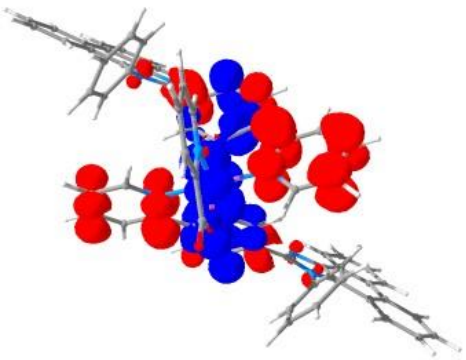

$S_0 \rightarrow S_1$

Donor	Acceptor			
	Ir	Pic	N-C	N-C
Ir	0.016	0.004	0.153	0.223
Pic	0.002	0.000	0.016	0.024
N-C	0.012	0.003	0.114	0.167
N-C	0.011	0.002	0.102	0.150

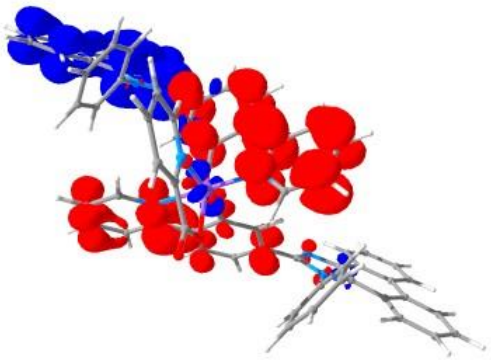

$S_0 \rightarrow S_2$

Donor	Acceptor			
	Ir	Pic	N-C	N-C
Ir	0.001	0.000	0.009	0.019
Pic	0.000	0.000	0.001	0.002
N-C	0.004	0.001	0.033	0.067
N-C	0.036	0.010	0.267	0.549

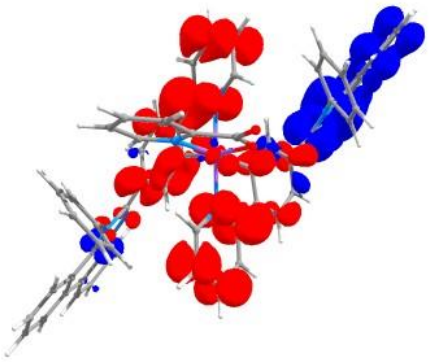

$S_0 \rightarrow S_3$

Donor	Acceptor			
	Ir	Pic	N-C	N-C
Ir	0.001	0.000	0.008	0.008
Pic	0.000	0.000	0.001	0.001
N-C	0.029	0.016	0.346	0.374
N-C	0.008	0.005	0.098	0.106

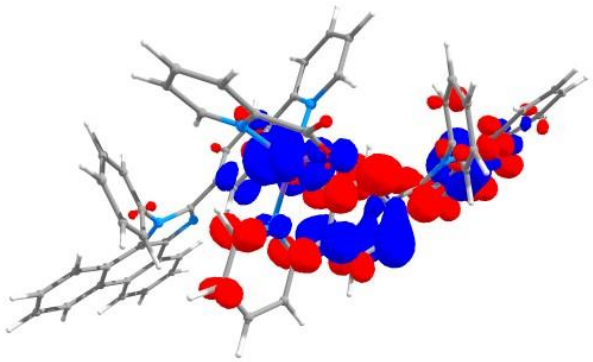

$S_0 \rightarrow S_4$

Donor	Acceptor			
	Ir	Pic	N-C	N-C
Ir	0.006	0.006	0.110	0.039
Pic	0.001	0.001	0.012	0.004
N-C	0.020	0.020	0.401	0.141
N-C	0.008	0.008	0.166	0.058

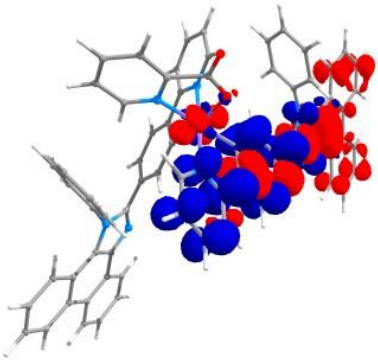

$T_1 \rightarrow S_0$

Donor	Acceptor			
	Ir	Pic	N-C	N-C
Ir	0.003	0.000	0.034	0.001
Pic	0.001	0.000	0.007	0.000
N-C	0.066	0.005	0.848	0.022
N-C	0.001	0.000	0.013	0.000

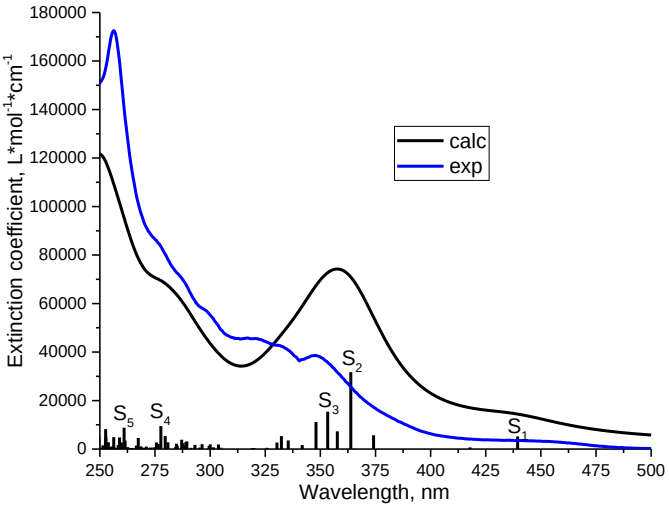

*Figure S19. Absorption spectra of {**1**+2H$^+$} in CH_2Cl_2 solution: experimental (blue) and calculated (black) lines with oscillator strengths of electronic transitions (bars).*

*Table S7. Table 1. Experimental and calculated absorption maxima (λ), extinction coefficients (ε), oscillator strengths (f) {**1**+2H$^+$}.*

Complex	λ_{abs}, nm (exp)	$\varepsilon*10^{-3}$, $L*mol^{-1}*cm^{-1}$ (exp)	Transitions	λ_{abs}, nm (calc)	*f* (calc)	Contribution of main NTO pair in transition (%)
{**1**+2H$^+$}	256	172	S_0-S_5	261	0.18	28
	277sh	84	S_0-S_4	278	0.19	59
	348	39	S_0-S_3	353	0.31	63
			S_0-S_2	364	0.65	61
	450sh	4	S_0-S_1	439	0.11	95

*Table S8. The decrease (blue) and increase (red) in electron density for most intensive electronic absorption transitions of {**1**+2H$^+$}. The data for the corresponding interfragment charge transfer (IFCT) are given below the figures. Diagonal values represent intraligand transitions, off-diagonal values represent a charge transfer from "Donor" to "Acceptor".*

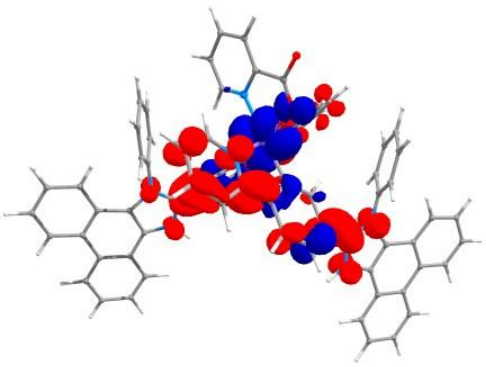

$S_0 \rightarrow S_1$

Donor	Acceptor			
	Ir	Pic	N-C	N-C
Ir	0.013	0.001	0.247	0.157
Pic	0.002	0.000	0.030	0.019
N-C	0.009	0.001	0.164	0.104
N-C	0.008	0.001	0.151	0.096

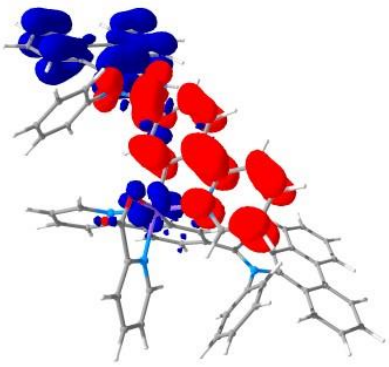

$S_0 \rightarrow S_2$

Donor	Acceptor			
	Ir	Pic	N-C	N-C
Ir	0.007	0.001	0.157	0.082
Pic	0.002	0.000	0.043	0.023
N-C	0.017	0.002	0.401	0.210
N-C	0.001	0.000	0.034	0.018

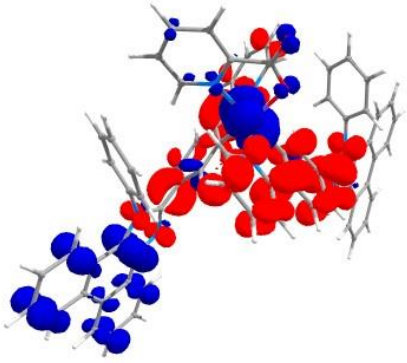

$S_0 \rightarrow S_3$

Donor	Acceptor			
	Ir	Pic	N-C	N-C
Ir	0.012	0.001	0.214	0.184
Pic	0.003	0.000	0.049	0.042
N-C	0.004	0.000	0.065	0.056
N-C	0.011	0.001	0.193	0.166

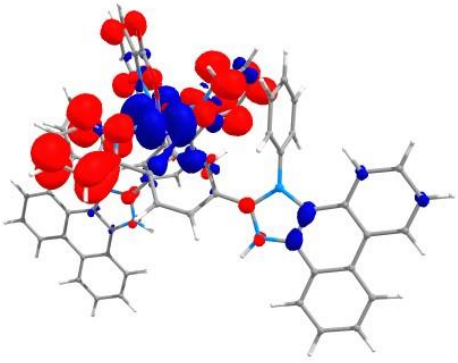

$S_0 \rightarrow S_4$

Donor	Acceptor			
	Ir	Pic	N-C	N-C
Ir	0.010	0.055	0.210	0.214
Pic	0.002	0.010	0.040	0.041
N-C	0.004	0.023	0.088	0.089
N-C	0.004	0.024	0.092	0.094

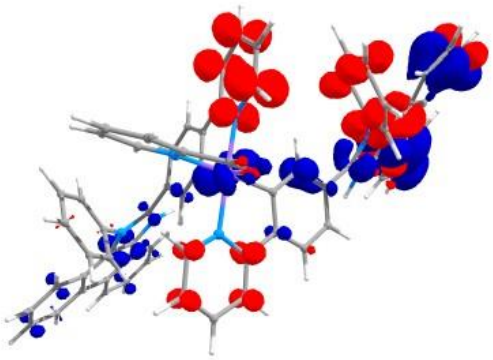

$S_0 \rightarrow S_5$

Donor	Acceptor			
	Ir	Pic	N-C	N-C
Ir	0.002	0.002	0.073	0.020
Pic	0.000	0.000	0.014	0.004
N-C	0.012	0.012	0.511	0.141
N-C	0.004	0.004	0.158	0.044

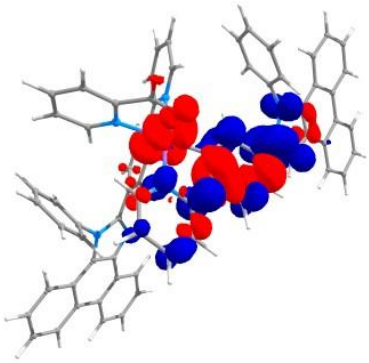

$T_1 \rightarrow S_0$

Donor	Acceptor			
	Ir	Pic	N-C	N-C
Ir	0.007	0.001	0.020	0.002
Pic	0.000	0.000	0.001	0.000
N-C	0.218	0.032	0.635	0.049
N-C	0.008	0.001	0.024	0.002

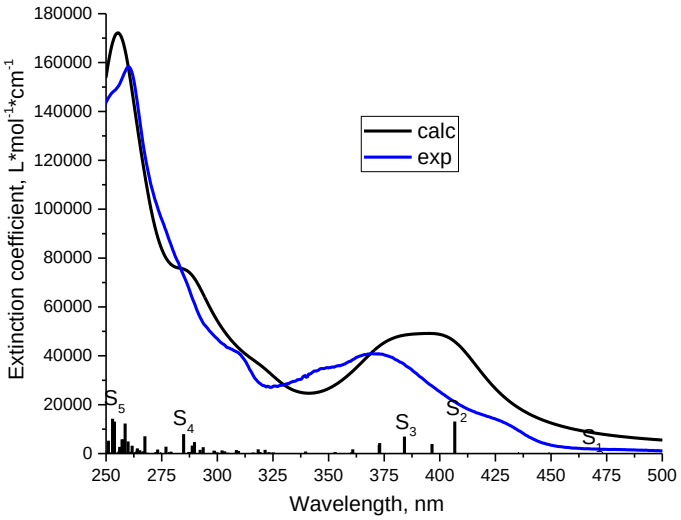

*Figure S20. Absorption spectra of complex **2** in CH_2Cl_2 solution: experimental (blue) and calculated (black) lines with oscillator strengths of electronic transitions (bars).*

*Table S9. Experimental and calculated absorption maxima (λ), extinction coefficients (ε), oscillator strengths (f) of **2**.*

Complex	λ_{abs}, nm (exp)	$\varepsilon*10^{-3}$, $L*mol^{-1}*cm^{-1}$ (exp)	Transitions	λ_{abs}, nm (calc)	*f* (calc)	Contribution of main NTO pair in transition (%)
2	260	149	S_0-S_5	253	0.48	35
	309sh	40	S_0-S_4	285	0.27	45
	370	41	S_0-S_3	384	0.24	92
	425sh	15	S_0-S_2	407	0.44	97
			S_0-S_1	473	0	99

*Table S10. The decrease (blue) and increase (red) in electron density for most intensive electronic absorption transitions of **2**. The data for the corresponding interfragment charge transfer (IFCT) are given below the figures. Diagonal values represent intraligand transitions, off-diagonal values represent a charge transfer from "Donor" to "Acceptor".*

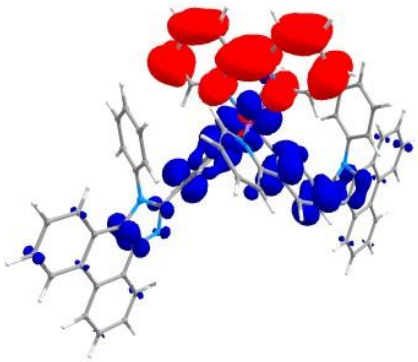

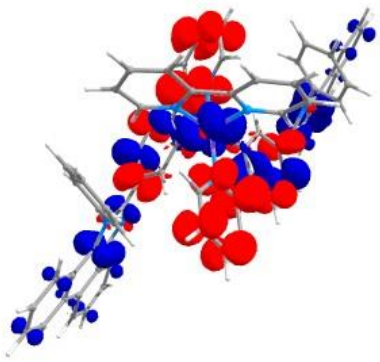

$S_0 \rightarrow S_1$

Donor	Acceptor			
	Ir	NN	N-C	N-C
Ir	0.009	0.244	0.001	0.001
NN	0.001	0.015	0.000	0.000
N-C	0.013	0.348	0.002	0.002
N-C	0.013	0.349	0.002	0.002

$S_0 \rightarrow S_2$

Donor	Acceptor			
	Ir	NN	N-C	N-C
Ir	0.008	0.001	0.086	0.086
NN	0.001	0.000	0.006	0.006
N-C	0.018	0.002	0.191	0.191
N-C	0.018	0.002	0.192	0.192

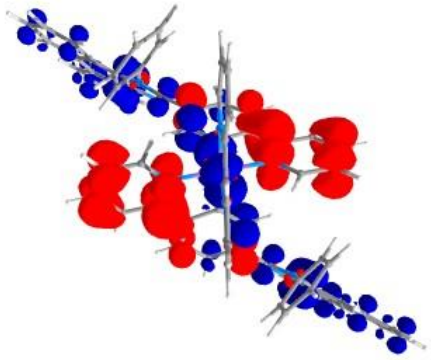

$S_0 \rightarrow S_3$

Donor	Acceptor			
	Ir	NN	N-C	N-C
Ir	0.009	0.001	0.095	0.095
NN	0.001	0.000	0.006	0.006
N-C	0.018	0.002	0.187	0.187
N-C	0.018	0.002	0.187	0.187

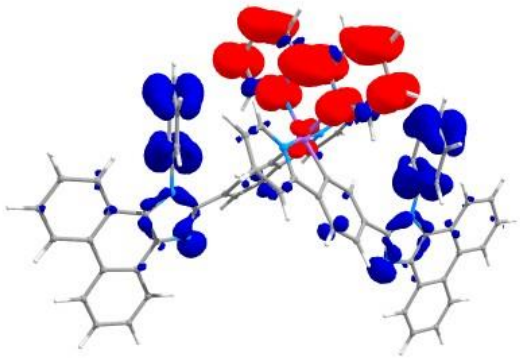

$S_0 \rightarrow S_4$

Donor	Acceptor			
	Ir	NN	N-C	N-C
Ir	0.008	0.203	0.025	0.025
NN	0.004	0.099	0.012	0.012
N-C	0.009	0.237	0.030	0.030
N-C	0.009	0.237	0.030	0.030

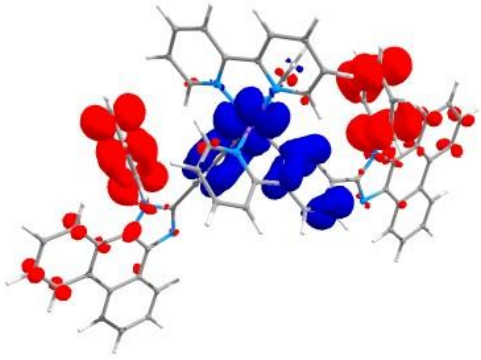

$S_0 \rightarrow S_5$

Donor	Acceptor			
	Ir	NN	N-C	N-C
Ir	0.002	0.007	0.076	0.076
NN	0.000	0.000	0.005	0.005
N-C	0.005	0.018	0.196	0.195
N-C	0.005	0.018	0.196	0.195

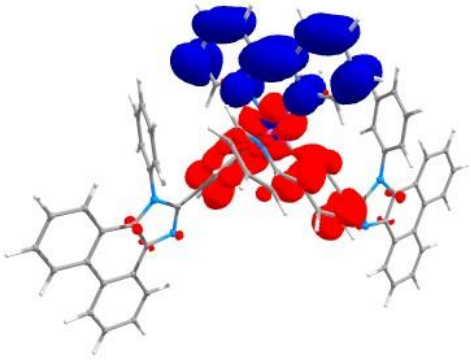

$T_1 \rightarrow S_0$

Donor	Acceptor			
	Ir	NN	N-C	N-C
Ir	0.011	0.001	0.012	0.012
NN	0.291	0.023	0.320	0.320
N-C	0.001	0.000	0.002	0.002
N-C	0.001	0.000	0.002	0.002

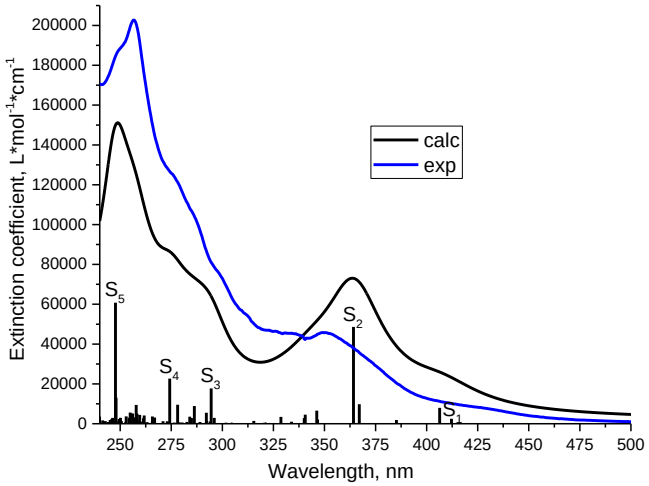

*Figure S21. Absorption spectra of {**2**+2H$^+$} in CH_2Cl_2 solution: experimental (blue) and calculated (black) lines with oscillator strengths of electronic transitions (bars).*

*Table S11. Experimental and calculated absorption maxima (λ), extinction coefficients (ε), oscillator strengths (f) {**2**+2H$^+$}.*

Complex	λ_{abs}, nm (exp)	$\varepsilon*10^{-3}$, $L*mol^{-1}*cm^{-1}$ (exp)	Transitions	λ_{abs}, nm (calc)	*f* (calc)	Contribution of main NTO pair in transition (%)
{**2**+2H$^+$}	257	202	S_0-S_5	248	1.07	33
	275sh	124	S_0-S_4	274	0.40	36
	300sh	72	S_0-S_3	295	0.31	74
	350	46	S_0-S_2	364	0.86	75
	425sh	8	S_0-S_1	412	0.04	96

*Table S12. The decrease (blue) and increase (red) in electron density for most intensive electronic absorption transitions of {**2**+2H$^+$}. The data for the corresponding interfragment charge transfer (IFCT) are given below the figures. Diagonal values represent intraligand transitions, off-diagonal values represent a charge transfer from "Donor" to "Acceptor".*

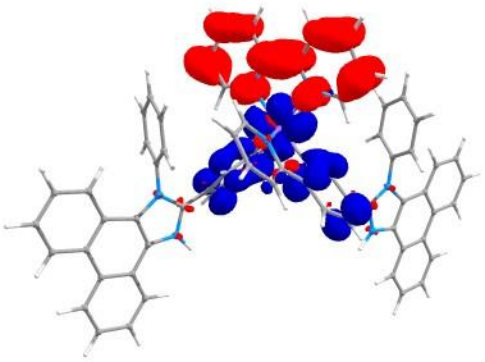

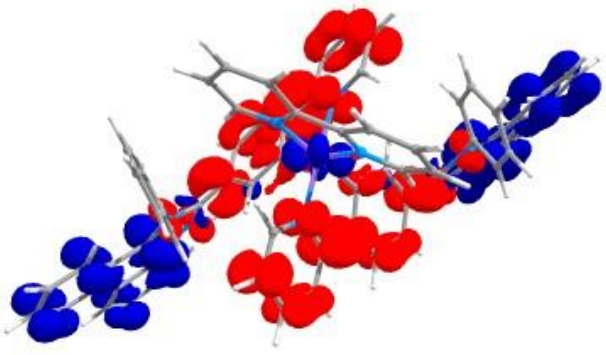

$S_0 \rightarrow S_1$

Donor	Acceptor			
	Ir	NN	N-C	N-C
Ir	0.019	0.282	0.046	0.046
NN	0.001	0.017	0.003	0.003
N-C	0.014	0.210	0.034	0.034
N-C	0.014	0.210	0.034	0.034

$S_0 \rightarrow S_2$

Donor	Acceptor			
	Ir	NN	N-C	N-C
Ir	0.001	0.001	0.020	0.020
NN	0.000	0.000	0.001	0.001
N-C	0.016	0.008	0.227	0.227
N-C	0.016	0.008	0.227	0.227

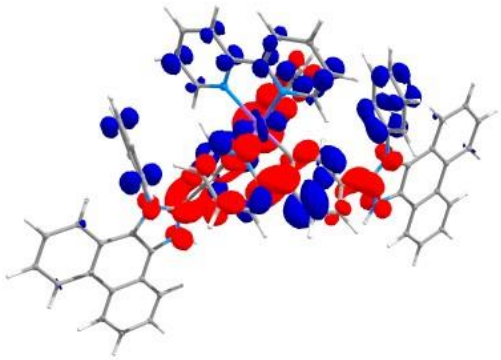

$S_0 \rightarrow S_3$

Donor	Acceptor			
	Ir	NN	N-C	N-C
Ir	0.002	0.001	0.034	0.034
NN	0.004	0.001	0.054	0.054
N-C	0.013	0.003	0.196	0.196
N-C	0.013	0.003	0.196	0.196

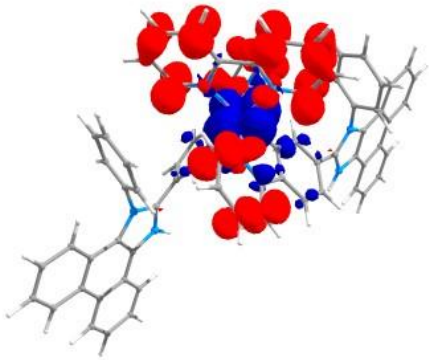

$S_0 \rightarrow S_4$

Donor	Acceptor			
	Ir	NN	N-C	N-C
Ir	0.007	0.127	0.115	0.115
NN	0.002	0.046	0.041	0.041
N-C	0.005	0.089	0.080	0.080
N-C	0.005	0.089	0.080	0.080

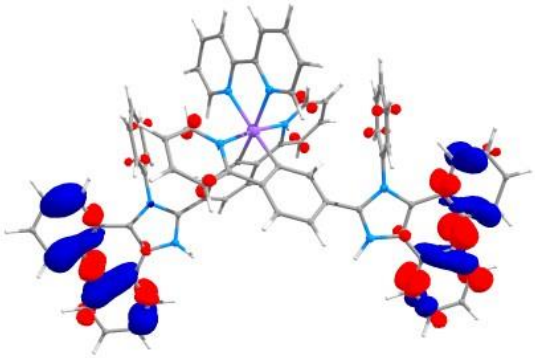

$S_0 \rightarrow S_5$

Donor	Acceptor			
	Ir	NN	N-C	N-C
Ir	0.000	0.000	0.008	0.008
NN	0.000	0.000	0.001	0.001
N-C	0.001	0.010	0.240	0.240
N-C	0.001	0.010	0.240	0.240

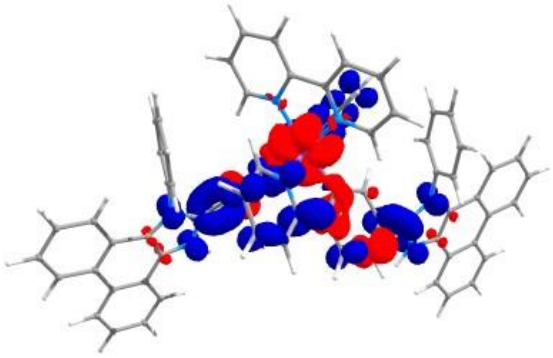

$T_1 \rightarrow S_0$

Donor	Acceptor			
	Ir	NN	N-C	N-C
Ir	0.010	0.001	0.013	0.013
NN	0.002	0.000	0.003	0.003
N-C	0.126	0.012	0.169	0.169
N-C	0.127	0.012	0.170	0.170

*Table S13. Partial protonation of complexes **1** and **2**: left – calculated absorption spectra for complexes **1** and **2** and their mono- and di-protonated forms, central and right: the decrease (blue) and increase (red) in electron density for absorption and emission transitions in mono-protonated forms.*

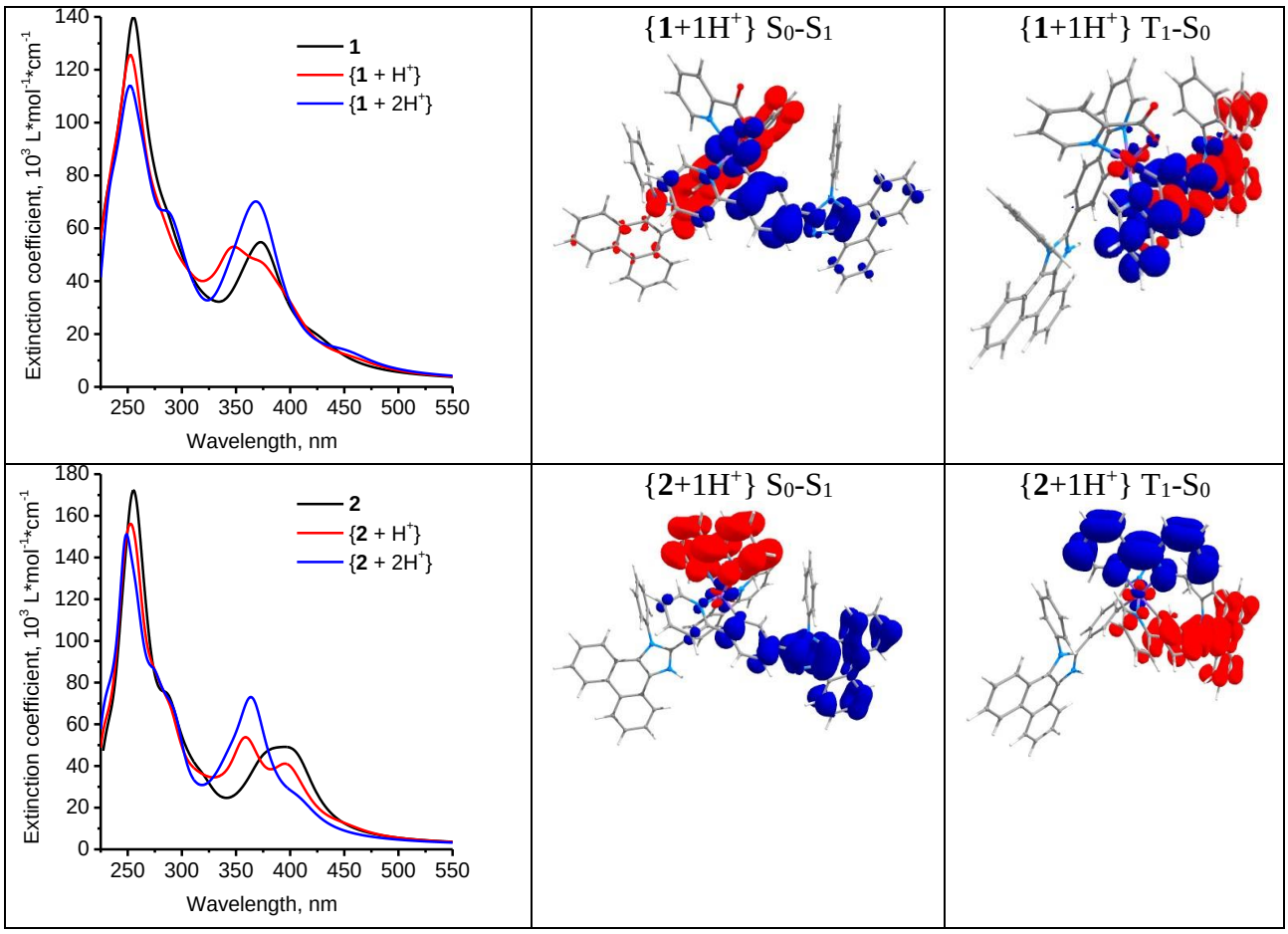

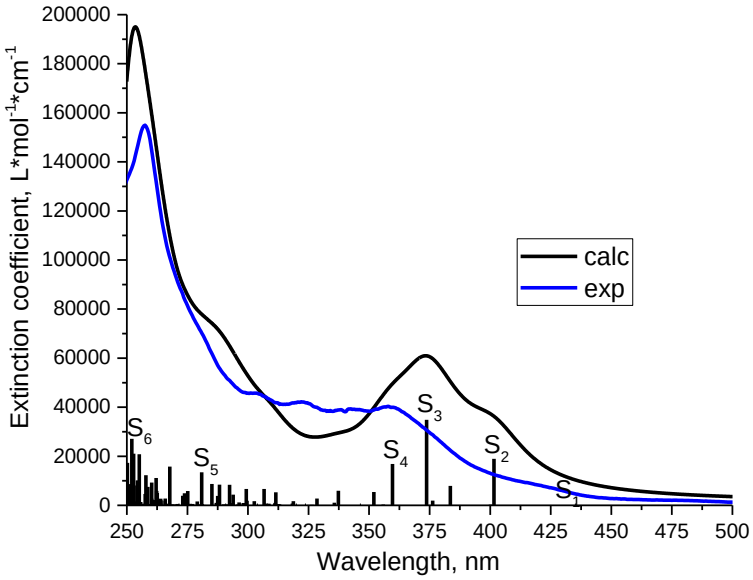

*Figure S22. Absorption spectra of complex {**3**-2H⁺} (deprotonated at the **N^N** ligand form of **3**) in CH_3OH: experimental (blue) and calculated (black) lines with oscillator strengths of electronic transitions (bars).*

*Table S14. Experimental and calculated absorption maxima (λ), extinction coefficients (ε), oscillator strengths (f) {**3**-2H$^+$}.*

Complex	λ_{abs}, nm (exp)	$\varepsilon*10^{-3}$, $L*mol^{-1}*cm^{-1}$ (exp)	Transitions	λ_{abs}, nm (calc)	*f* (calc)	Contribution of main NTO pair in transition (%)
{**3**-2H$^+$}	258	155	S_0-S_6	252	0.37	29
	304	45	S_0-S_5	281	0.18	52
	357	40	S_0-S_4	360	0.23	88
			S_0-S_3	374	0.47	90
	420sh	8	S_0-S_2	402	0.26	95
	480sh	2	S_0-S_1	435	0.00	98

*Table S15. The decrease (blue) and increase (red) in electron density for most intensive electronic absorption transitions of {**3**-2H$^+$}. The data for the corresponding interfragment charge transfer (IFCT) are given below the figures. Diagonal values represent intraligand transitions, off-diagonal values represent a charge transfer from "Donor" to "Acceptor".*

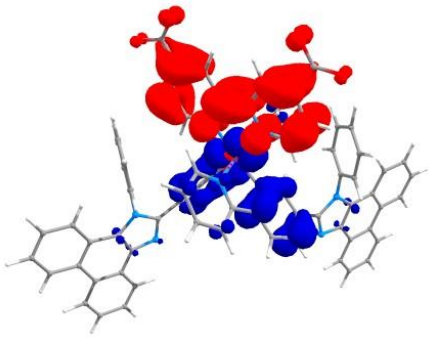

$S_0 \rightarrow S_1$

Donor	Acceptor			
	Ir	NN	N-C	N-C
Ir	0.013	0.323	0.002	0.002
NN	0.001	0.021	0.000	0.000
N-C	0.013	0.302	0.002	0.002
N-C	0.013	0.302	0.002	0.002

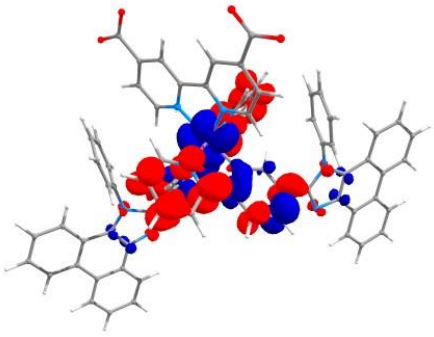

$S_0 \rightarrow S_2$

Donor	Acceptor			
	Ir	NN	N-C	N-C
Ir	0.014	0.001	0.150	0.150
NN	0.001	0.000	0.010	0.010
N-C	0.015	0.001	0.158	0.158
N-C	0.015	0.001	0.158	0.158

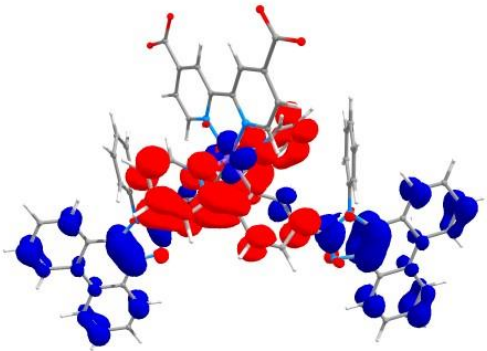

$S_0 \rightarrow S_3$

Donor	Acceptor			
	Ir	NN	N-C	N-C
Ir	0.004	0.000	0.042	0.042
NN	0.000	0.000	0.003	0.003
N-C	0.020	0.002	0.216	0.216
N-C	0.020	0.002	0.216	0.216

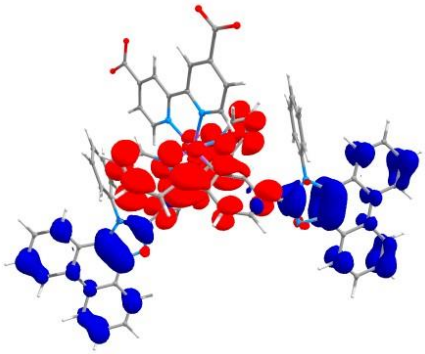

$S_0 \rightarrow S_4$

Donor	Acceptor			
	Ir	NN	N-C	N-C
Ir	0.000	0.000	0.004	0.004
NN	0.000	0.000	0.000	0.000
N-C	0.021	0.003	0.236	0.236
N-C	0.021	0.003	0.236	0.236

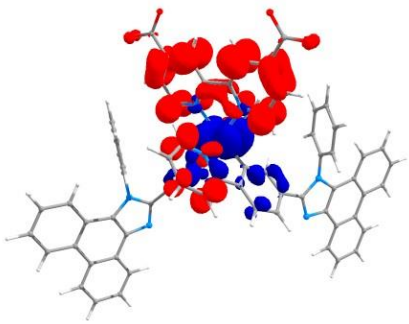

$S_0 \rightarrow S_5$

Donor	Acceptor			
	Ir	NN	N-C	N-C
Ir	0.010	0.240	0.070	0.070
NN	0.003	0.079	0.023	0.023
N-C	0.006	0.149	0.043	0.043
N-C	0.006	0.148	0.043	0.043

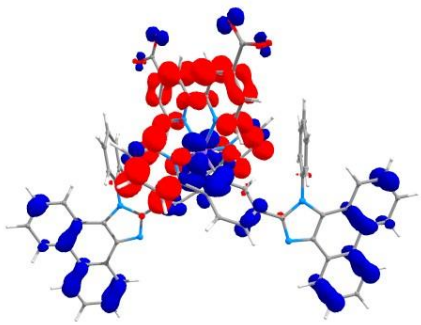

$S_0 \rightarrow S_6$

Donor	Acceptor			
	Ir	NN	N-C	N-C
Ir	0.003	0.037	0.031	0.031
NN	0.005	0.061	0.050	0.050
N-C	0.011	0.134	0.110	0.110
N-C	0.011	0.134	0.111	0.111

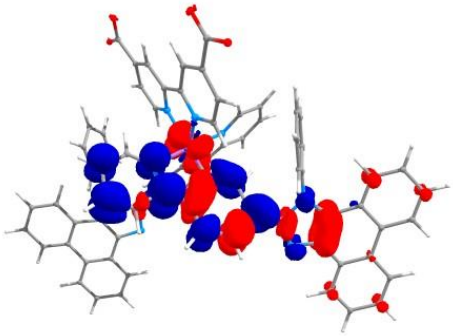

$T_1 \rightarrow S_0$

Donor	Acceptor			
	Ir	NN	N-C	N-C
Ir	0.008	0.001	0.004	0.031
NN	0.003	0.000	0.001	0.010
N-C	0.008	0.001	0.004	0.031
N-C	0.160	0.022	0.079	0.638

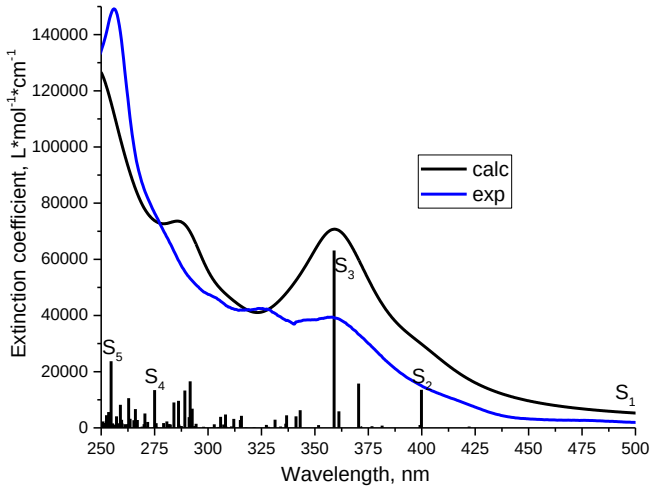

*Figure S23. Absorption spectra of complex {**3**+2H$^+$} in CH_3OH: experimental (blue) and calculated (black) lines with oscillator strengths of electronic transitions (bars).*

*Table S16 Experimental and calculated absorption maxima (λ), extinction coefficients (ε), oscillator strengths (f) {**3**+2H$^+$}.*

Complex	λ_{abs}, nm (exp)	$\varepsilon*10^{-3}$, $L*mol^{-1}*cm^{-1}$ (exp)	Transitions	λ_{abs}, nm (calc)	*f* (calc)	Contribution of main NTO pair in transition (%)
{**3**+2H$^+$}	255	148	S_0-S_5	254	0.32	41
			S_0-S_4	275	0.18	36
	357	40	S_0-S_3	359	0.86	75
	420sh	9	S_0-S_2	400	0.18	88
	480sh	2	S_0-S_1	496	0.00	99

.

*Table S17. The decrease (blue) and increase (red) in electron density for most intensive electronic absorption transitions of {**3**+2H$^+$}. The data for the corresponding interfragment charge transfer (IFCT) are given below the figures. Diagonal values represent intraligand transitions, off-diagonal values represent a charge transfer from "Donor" to "Acceptor".*

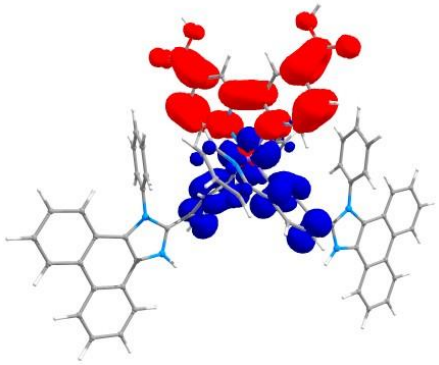

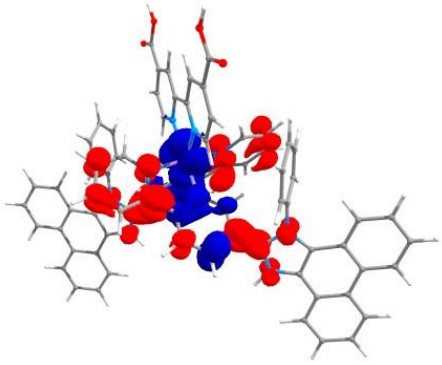

$S_0 \rightarrow S_1$

Donor	Acceptor			
	Ir	NN	N-C	N-C
Ir	0.016	0.357	0.002	0.002
NN	0.001	0.022	0.000	0.000
N-C	0.013	0.284	0.002	0.002
N-C	0.013	0.284	0.002	0.002

$S_0 \rightarrow S_2$

Donor	Acceptor			
	Ir	NN	N-C	N-C
Ir	0.014	0.033	0.171	0.171
NN	0.001	0.002	0.011	0.011
N-C	0.011	0.025	0.128	0.129
N-C	0.011	0.025	0.129	0.129

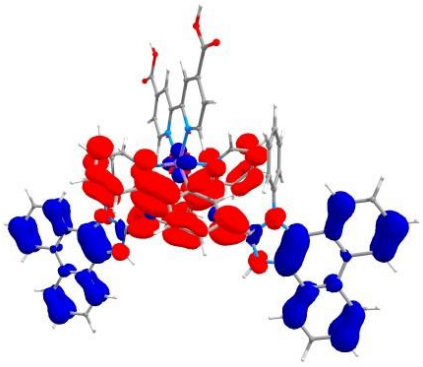

$S_0 \rightarrow S_3$

Donor	Acceptor			
	Ir	NN	N-C	N-C
Ir	0.001	0.000	0.016	0.016
NN	0.000	0.000	0.001	0.001
N-C	0.017	0.005	0.230	0.230
N-C	0.017	0.005	0.230	0.230

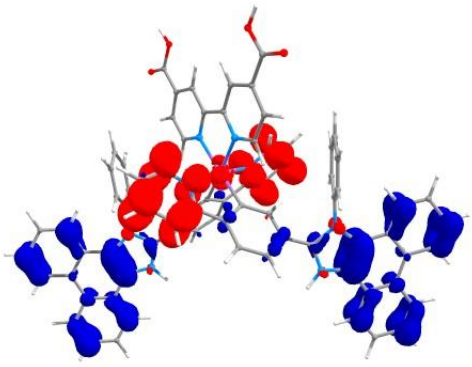

$S_0 \rightarrow S_4$

Donor	Acceptor			
	Ir	NN	N-C	N-C
Ir	0.003	0.007	0.052	0.052
NN	0.001	0.001	0.011	0.011
N-C	0.011	0.027	0.197	0.197
N-C	0.011	0.027	0.197	0.197

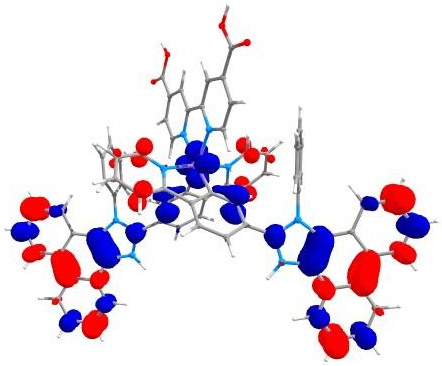

$S_0 \rightarrow S_5$

Donor	Acceptor			
	Ir	NN	N-C	N-C
Ir	0.000	0.000	0.029	0.029
NN	0.000	0.000	0.002	0.002
N-C	0.004	0.002	0.234	0.234
N-C	0.003	0.002	0.229	0.229

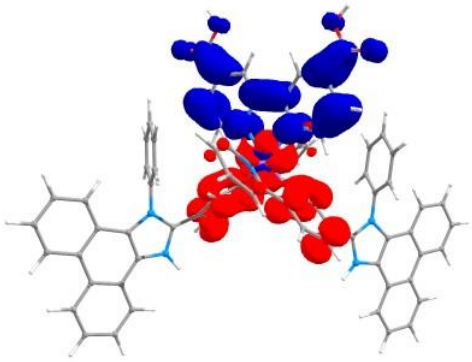

$T_1 \rightarrow S_0$

Donor	Acceptor			
	Ir	NN	N-C	N-C
Ir	0.017	0.001	0.014	0.014
NN	0.340	0.029	0.287	0.287
N-C	0.002	0.000	0.002	0.002
N-C	0.002	0.000	0.002	0.002

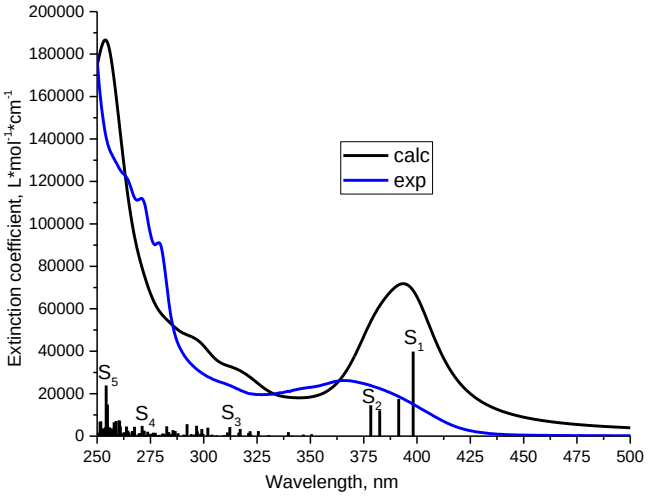

*Figure S24. Absorption spectra of **4** in water: experimental (blue) and calculated (black) lines with oscillator strengths of electronic transitions (bars).*

*Table S18. Experimental and calculated absorption maxima (λ), extinction coefficients (ε), oscillator strengths (f) **4**.*

Complex	λ_{abs}, nm (exp)	$\varepsilon*10^{-3}$, $L*mol^{-1}*cm^{-1}$ (exp)	Transitions	λ_{abs}, nm (calc)	*f* (calc)	Contribution of main NTO pair in transition (%)
4	263sh	128	S_0-S_5	255	0.20	27
	271	117	S_0-S_4	271	0.07	36
	308sh	25	S_0-S_3	312	0.06	53
	367	27	S_0-S_2	378	0.20	97
			S_0-S_1	398	0.54	94

*Table S19. The decrease (blue) and increase (red) in electron density for most intensive electronic absorption transitions of **4**. The data for the corresponding interfragment charge transfer (IFCT) are given below the figures. Diagonal values represent intraligand transitions, off-diagonal values represent a charge transfer from "Donor" to "Acceptor".*

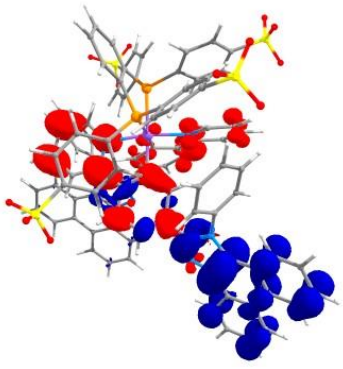

$S_0 \rightarrow S_1$

Donor	Acceptor			
	Ir	PP	N-C	N-C
Ir	0.000	0.000	0.005	0.002
PP	0.000	0.000	0.004	0.001
N-C	0.021	0.036	0.616	0.190
N-C	0.003	0.005	0.089	0.027

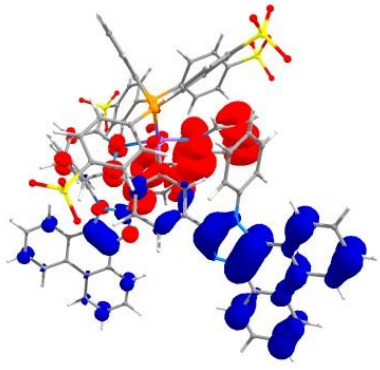

$S_0 \rightarrow S_2$

Donor	Acceptor			
	Ir	PP	N-C	N-C
Ir	0.000	0.000	0.000	0.002
PP	0.000	0.000	0.001	0.003
N-C	0.016	0.030	0.114	0.532
N-C	0.007	0.013	0.050	0.232

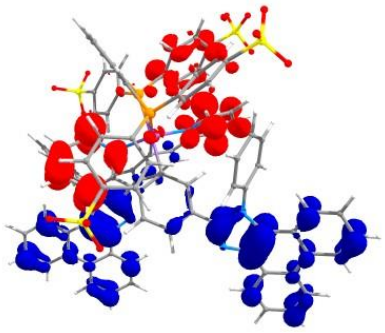

$S_0 \rightarrow S_3$

Donor	Acceptor			
	Ir	PP	N-C	N-C
Ir	0.001	0.009	0.010	0.012
PP	0.000	0.003	0.003	0.004
N-C	0.017	0.110	0.129	0.146
N-C	0.023	0.152	0.179	0.203

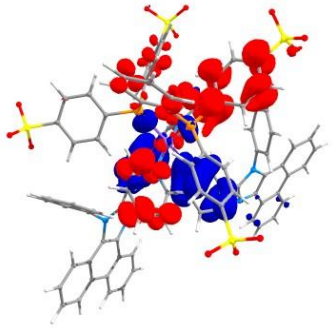

$S_0 \rightarrow S_4$

Donor	Acceptor			
	Ir	PP	N-C	N-C
Ir	0.001	0.019	0.007	0.008
PP	0.005	0.086	0.031	0.036
N-C	0.010	0.178	0.065	0.074
N-C	0.015	0.261	0.096	0.109

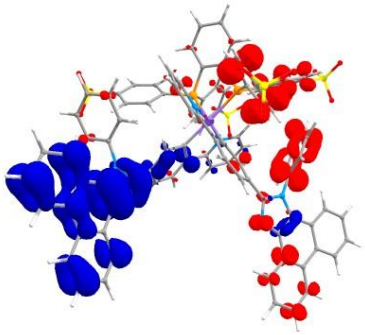

$S_0 \rightarrow S_5$

Donor	Acceptor			
	Ir	PP	N-C	N-C
Ir	0.000	0.009	0.012	0.006
PP	0.000	0.013	0.017	0.009
N-C	0.003	0.099	0.132	0.066
N-C	0.007	0.210	0.278	0.139

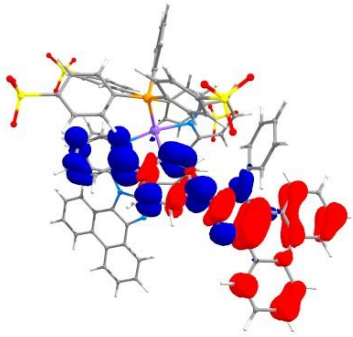

$T_1 \rightarrow S_0$

Donor	Acceptor			
	Ir	PP	N-C	N-C
Ir	0.000	0.000	0.000	0.014
PP	0.000	0.000	0.000	0.021
N-C	0.000	0.000	0.000	0.022
N-C	0.009	0.003	0.005	0.926

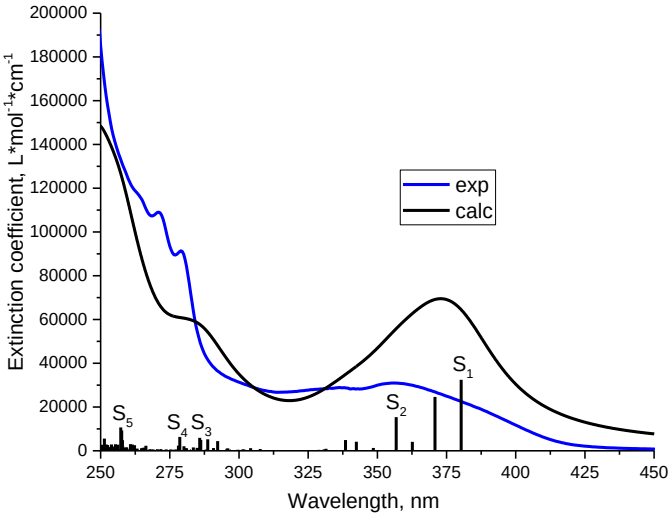

*Figure S25. Absorption spectra of {**4**+2H$^+$} in water: experimental (blue) and calculated (black) lines with oscillator strengths of electronic transitions (bars).*

*Table S20. Experimental and calculated absorption maxima (λ), extinction coefficients (ε), oscillator strengths (f) {**4**+2H$^+$}.*

Complex	λ_{abs}, nm (exp)	$\varepsilon*10^{-3}$, $L*mol^{-1}*cm^{-1}$ (exp)	Transitions	λ_{abs}, nm (calc)	*f* (calc)	Contribution of main NTO pair in transition (%)
{**4**+2H$^+$}	264sh	117	S_0-S_5	257	0.19	28
	271	110	S_0-S_4	279	0.11	41
	279	91	S_0-S_3	286	0.10	58
	357	31	S_0-S_2	357	0.27	70
			S_0-S_1	380	0.57	92

*Table S21. The decrease (blue) and increase (red) in electron density for most intensive electronic absorption transitions of {**4**+2H$^+$}. The data for the corresponding interfragment charge transfer (IFCT) are given below the figures. Diagonal values represent intraligand transitions, off-diagonal values represent a charge transfer from "Donor" to "Acceptor".*

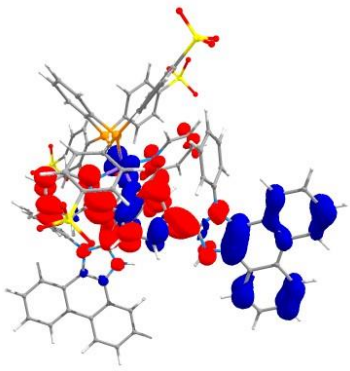

$S_0 \rightarrow S_1$

Donor	Acceptor			
	Ir	PP	N-C	N-C
Ir	0.001	0.002	0.059	0.029
PP	0.001	0.001	0.025	0.012
N-C	0.010	0.018	0.440	0.215
N-C	0.003	0.005	0.121	0.059

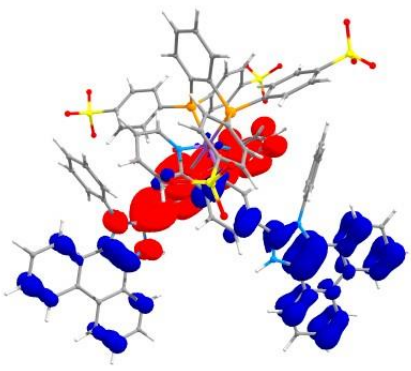

$S_0 \rightarrow S_2$

Donor	Acceptor			
	Ir	PP	N-C	N-C
Ir	0.001	0.001	0.017	0.040
PP	0.001	0.001	0.009	0.020
N-C	0.010	0.013	0.162	0.379
N-C	0.006	0.008	0.100	0.233

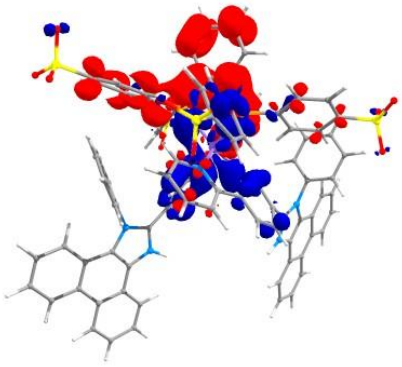

$S_0 \rightarrow S_3$

Donor	Acceptor			
	Ir	PP	N-C	N-C
Ir	0.002	0.034	0.015	0.006
PP	0.016	0.225	0.100	0.038
N-C	0.017	0.240	0.106	0.040
N-C	0.007	0.095	0.042	0.016

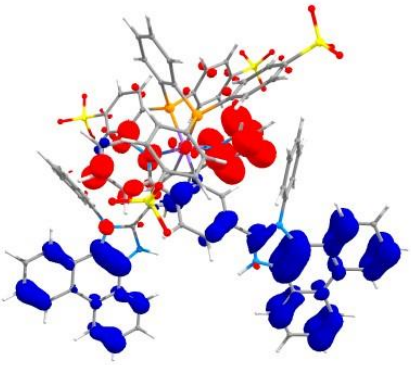

$S_0 \rightarrow S_4$

Donor	Acceptor			
	Ir	PP	N-C	N-C
Ir	0.002	0.013	0.008	0.025
PP	0.002	0.016	0.009	0.030
N-C	0.018	0.133	0.077	0.250
N-C	0.015	0.116	0.067	0.219

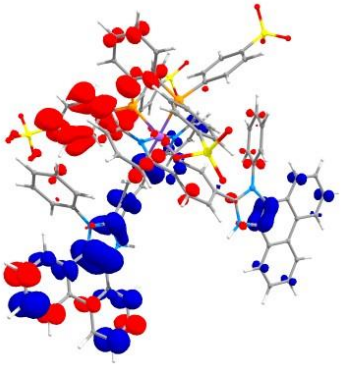

$S_0 \rightarrow S_5$

Donor	Acceptor			
	Ir	PP	N-C	N-C
Ir	0.000	0.006	0.005	0.009
PP	0.000	0.008	0.008	0.012
N-C	0.004	0.082	0.081	0.130
N-C	0.009	0.181	0.178	0.286

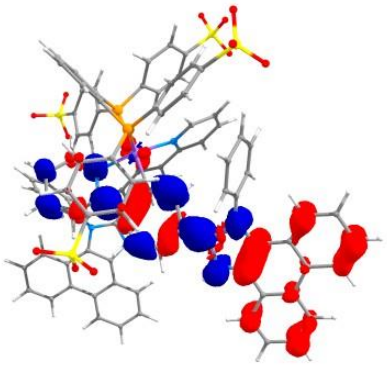

$T_1 \rightarrow S_0$

Donor	Acceptor			
	Ir	PP	N-C	N-C
Ir	0.000	0.001	0.013	0.000
PP	0.001	0.001	0.017	0.000
N-C	0.027	0.039	0.869	0.012
N-C	0.001	0.001	0.018	0.000